Double structure hydromechanical coupling formalism and a model for unsaturated expansive clays

David Mašín, *Charles University in Prague, Czech Republic*

corresponence to:
David Mašín
Charles University in Prague
Faculty of Science
Albertov 6
12843 Prague 2, Czech Republic
E-mail: masin@natur.cuni.cz
Tel: +420-2-2195 1552, Fax: +420-2-2195 1556

February 3, 2012

Manuscript submitted to the journal *Engineering Geology*,
special issue
"Unsaturated soils: Theory and Applications"

Abstract

A formalism for double structure hydromechanical coupled modelling of aggregated unsaturated soils has been developed. Independent coupled hydromechanical models are considered for each structural level, including independent measures of macromechanical and micromechanical effective stresses. The models are linked using a coupling function to obtain the global response. The individual components have been selected to represent the behaviour of compacted expansive clays. The macrostructural mechanical model is based on the existing hypoplastic model for unsaturated soils. Hydromechanical coupling at each structural level is efficiently achieved by linking the effective stress formulation with the water retention model. An essential component of the model is representation of microstructural swelling. It is demonstrated that its calibration on wetting induced expansion measured in oedometric (mechanical) tests leads to a correct global hydraulic response, providing a supporting argument for the adopted coupling approach. An interesting consequence of the model formulation is that it does not suffer from volumetric rachetting, which is often regarded as one of the main drawbacks of hypoplasticity. The proposed model has a small number of material parameters. Its predictive capabilities have been confirmed by simulation of comprehensive experimental data set on compacted Boom clay.

Keywords: expansive soils; double structure; unsaturated soils; hypoplasticity; hydromechanical behaviour; water retention curve

1 Introduction

Advances in understanding of the behaviour of expansive compacted soils, gained over the last 20 years, reveal a crucial role of microstructure in modelling of their behaviour. The soil compacted dry of optimum has a structure with two distinct pore systems. Gens and Alonso (1992) and Alonso et al. (1999) developed a pioneering mechanical model for expansive clays, which combined an existing model for unsaturated soils with low plasticity with a simple reversible model for microstructure, linked by a coupling function. The role of microstructure in the soil hydraulic behaviour has been understood by Romero (1999) and Romero et al. (1999), and recently combined into a complete water retention model by Romero et al. (2011). The above two models considered separately two levels of structure and linked the responses using a coupling function. The first model focused on the mechanical behaviour (Alonso et al. 1999), while the second on the hydraulic behaviour (Romero et al. 2011).

From different perspective, recent past advances in modelling of the hydromechanical behaviour of unsaturated soils reveal crucial role of hydromechanical coupling. Volumetric deformation (mechanical response) of soil skeleton influences the degree of saturation and the air entry value of suction (hydraulic response), which in turn influence soil effective stress and thus affect its mechanical properties (see, e.g., models and discussion in D'Onza et al. 2011).

Following the above brief summary, expanded in Sec. 2, the behaviour of the two structural levels will be in this work considered as separate, linked by a suitable coupling function to obtained the global response. Such an approach is schematized in Fig. 1. The four partial constitutive models will be denoted as $\mathbf{G}^M$, $\mathbf{G}^m$, H^M and H^m (macrostructure and microstructure mechanical and hydraulic models respectively). The hydromechanical coupling mechanisms for microstructure and macrostructure are denoted as $\mathbf{G}^M H^M$ and $\mathbf{G}^m H^m$ respectively.

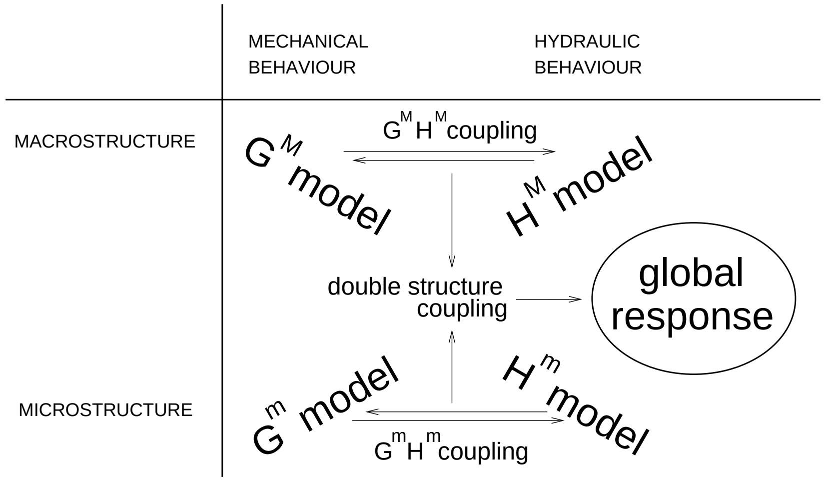

Figure 1: Schematic representation of the modelling approach adopted in this paper.

Existing constitutive models for double structure soils can be divided into two main groups. Models from the first group do not consider independent behaviour of macrostructure and microstructure, they are defined using global quantities. Sun and Sun (2011) developed such a model for expansive soils, considering full hydromechanical coupling. Cui et al. (2002) (realistically) assumed that the role of macroporosity in swelling of soils with dense structure may be neglected, and developed the global mechanical model based on the microstructural $\mathbf{G}^m$ model. Similarly, Koliji et al. (2008) and Najser et al. (2012) described the behaviour of double porosity lumpy soils using a model based on the microstructural behaviour ($\mathbf{G}^m$), with phenomenological incorporation of the influence of macrostructure.

The primary idea of this paper is to use separate formulations for the behaviour of macrostructure and microstructure. This approach is regarded as advantageous, as it is not necessary to search for a new and often intricate global constitutive model, and it is possible to use existing and well-evaluated models for each structural level. Success of the existing models considering double structure coupling supports this assumption. Soil mechanical behaviour has in this way been described by models by Gens and Alonso (1992), Alonso et al. (1999), Yang et al. (1998), Sánchez et al. (2005) and Thomas and Cleall (1999). Soil hydraulic behaviour by the model by Romero et al. (2011). Alonso et al. (2011) presented an advanced double structure based model considering all four $\mathbf{G}^M$, $\mathbf{G}^m$, H^M and H^m components. However, their model neglected the dependency of water retention behaviour on volumetric deformation ($\mathbf{G}^M H^M$ and $\mathbf{G}^m H^m$ couplings are thus not fully accounted for). Similar advanced model is attributed to Gens et al. (2011). Della Vecchia et al. (2011) developed a fully coupled hydro-mechanical model for double structure soils as an extension of the model by Romero et al. (2011). It considered all the above mentioned coupling mechanisms, different in details when compared to the present contribution.

One of the main means of hydromechanical coupling at each of the two structural levels is the definition of the effective stress (often linked to hydraulic quantities). All the above models use the effective stress defined in terms of global quantities. Thus, $\mathbf{G}^M$ and $\mathbf{G}^m$ cannot be considered as fully independent. This drawback can be eliminated by adopting an approach by Alonso et al. (2010), who suggested to attribute the main features (such as shear strength) of the double structure soil behaviour to the behaviour of macrostructure, and analyse it using effective stress measure independent of the microstructural quantities. Such an approach will be used throughout this work, for each structural level. Different approach has been suggested by Khalili et al. (2005) and Bagherieh et al. (2009). Based on the microstructural interpretation, they developed a formulation for the *global* effective stress within double porous medium. It may then be used within global constitutive equation, where independent consideration of the two structural levels is no-more needed. The double structure coupling mechanism has thus in their work been moved from the "external" double structure coupling function into the effective stress equation.

The structure of this paper is as follows. After summary of the behaviour of compacted expansive soils, a formal formulation of the double structure hydromechanical model based on fully independent models for the two structural levels is developed. In the next part of the paper, specific components of the proposed general model are selected so that they lead to a concise fully coupled model for expansive clays. The model is then evaluated using comprehensive experimental data on unsaturated compacted Boom clay by Romero (1999).

Notation and conventions: Compact tensorial notation is used throughout. Second-order tensors are denoted with bold letters (e.g. $\boldsymbol{\sigma}$, $\mathbf{N}$) and fourth-order tensors with calligraphic bold letters (e.g. $\boldsymbol{\mathcal{L}}$, $\boldsymbol{\mathcal{A}}$). Symbols "$\cdot$" and ":" between tensors of various orders denote inner product with single and double contraction, respectively. The dyadic product of two tensors is indicated by "$\otimes$", and $\|\dot{\boldsymbol{\epsilon}}\|$ represents the Euclidean norm of $\dot{\boldsymbol{\epsilon}}$. The trace operator is defined as $\operatorname{tr}\dot{\boldsymbol{\epsilon}} = \mathbf{1} : \dot{\boldsymbol{\epsilon}}$; $\mathbf{1}$ and $\boldsymbol{\mathcal{I}}$ denote second-order and fourth-order unity tensors, respectively. Following the sign convention of continuum mechanics, compression is taken as negative. However, Roscoe's variables $p = -\operatorname{tr}\boldsymbol{\sigma}/3$ and $\epsilon_v = -\operatorname{tr}\boldsymbol{\epsilon}$, and pore fluid and gas pressures u_w and u_a are defined to be positive in compression. The operator $\langle x \rangle$ denotes the positive part of any scalar function x, thus $\langle x \rangle = (x + |x|)/2$. The effective stress is denoted as $\boldsymbol{\sigma}$, net stress $\boldsymbol{\sigma}^{net} = \boldsymbol{\sigma}^{tot} + u_a$, where $\boldsymbol{\sigma}^{tot}$ is total stress. Matric suction is defined as $s = u_a - u_w$. Macrostructural quantities are denoted by superscript ^{M}, microstructural quantities by superscript ^{m}.

2 Double structure of expansive soils and its evolution with mechanical and hydraulic loading

It has now been well understood that the soil compacted dry of optimum has a structure with two distinct pore systems. The role of aggregated structure in constitutive modelling of the mechanical behaviour of unsaturated expansive soils has been recognised since the pioneering conceptual model by Gens and Alonso (1992), and later developed mathematical formalism by Alonso et al. (1999) (so-called BExM model). According to their approach, the behaviour of two structural levels may be considered separate, linked by coupling functions. Under the assumption of full saturation of the aggregates, they postulated that the deformation of the aggregates is purely volumetric and reversible, governed by the saturated effective mean stress $p = p^{net} + s$. The deformation of the macrostructure is governed by an existing model for unsaturated soils with low plasticity. Coupling between the two structural levels depends on the size of macropores (interaggregate pores). In soils with open macrostructure, aggregates during swelling invade the macropores, leading to the accumulated compression during cyclic changes of suction. Contrary, in soils with the initially closed macrostructure, macroporosity develops as a result of drying with less macropore invasion during wetting, leading to an accumulated expansion. In their development, Alonso et al. (1999) considered hydraulic and mechanical equilibrium between both levels of structure (both are subject to the same net stress and suction).

The different assumptions adopted in the above models have been subject of a detailed evaluation in a number subsequent studies. Microstructure evolution can be studied directly or indirectly. Among the direct methods, the most popular are mercury intrusion porosimetry (MIP) and environmental scanning electron microscopy (ESEM) (for complete review see Romero and Simms 2008). Indirect methods evaluate fabric evolution through measurement of the soil mechanical and water retention properties. A typical MIP result showing the development of microstructure with wetting is in Fig. 2a, with pore size density functions of a statically dry-of-optimum compacted London clay (Monroy et al. 2010). With decreasing suction, the microporosity increases, implying swelling of aggregates. The macroporosity, however, remains largely untouched, so the penetration of the aggregates into macropores is insignificant in this case. Only in the last step (wetting from suction 40 kPa to 0 kPa) the porosity becomes mono-modal, and the aggregated structure is not clear any more. Similar results were obtained by Lloret and Villar (2007), who reported also occlusion of macropores due to aggregate swelling. Romero et al. (2011) and Simms and Yanful (2001) observed that although the porosity is mono-modal upon saturation, the bi-modal porosity is recovered by subsequent drying. This process has been traced by Cuisinier and Laloui (2004) by testing compacted sandy loam along drying path (Fig. 2b). After re-establishment of the bi-modal pore size distribution, further drying caused reduction of macroporosity, with little influence on the microporosity (in fact, micropore volume slightly increased, as a result of closure of macrovoids which then added up to the microporosity). This has been confirmed by Romero et al. (2011), who dried the compacted Boom clay after saturation to very high suction (100 MPa). While the microporosity recovered to its original state, macroporosity was largely reduced.

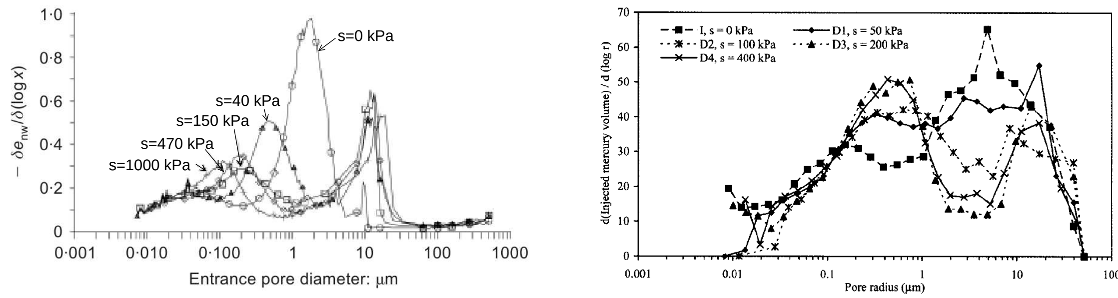

(a) (b)

Figure 2: (a) Development of microstructure of compacted London clay with wetting (Monroy et al. 2010, modified). (b) Microstructural changes of a compacted sandy loam during drying (Cuisinier and Laloui 2004).

Loading under constant suction or constant water content was studied by Sivakumar et al. (2006), Miao et al. (2007), Thom et al. (2007), Lloret and Villar (2007), Simms and Yanful (2001), Alonso et al. (2011), Romero et al. (2011), Romero and Simms (2008) and Cuisinier and Laloui (2004). They all reported that loading (compaction) influenced predominantly the macrovoids, which closed up with increasing load. Microporosity remained either untouched (Fig. 3a), or it slightly increased with increasing compaction effort (Fig. 3b). A possible interpretation is that upon high stress compaction a proportion of macrovoids closed up and thus added up to microporosity. Note that this result does not imply the aggregates to be undeformable with load. Rather, it implies that the aggregate deformation is reversible, as the porosity of the samples compacted to different stresses is measured on samples removed from the testing apparatuses, and thus on unloaded samples. Reversibility (though hysteretic) of the aggregate deformation subject to suction variation this time has also been confirmed by Romero and Simms (2008), who extracted the microscale volume change from the overall volume change by digital image analysis of ESEM micrographs.

Microstructural changes reported above are manifested in the soil response to hydromechanical loading. The aggregates swell upon wetting, but the overall soil volumetric behaviour depends on the amount of occlusion of macropores by aggregates and on the stability of the macrostructure. It, in turn, depends on the level of relative opening of the soil macrostructure (which increases with increasing void ratio and with increasing stress). Consequently, some authors report accumulated soil expansion with cyclic suction variation (for example, Gens and Alonso 1992, Romero and Simms 2008, Romero 1999) and some authors report accumulated compaction (e.g., Airò Farulla et al. 2010, Airò Farulla et al. 2007, Romero 1999). The magnitude of swelling/compaction depends on the stress level and void ratio (Airò Farulla et al. 2007, Romero 1999, Alonso et al. 1995, Taibi et al. 2011, Villar 1999). It is also important to recognise that the magnitude of swelling depends, from the quantitative point of view, not only on the level of occlusion of macropores by aggregates, but also on the stress level dependency of swelling of individual aggregates. This issue requires considerable attention, as important portion of the overall aggregate volume change is related to the physico-chemical phenomena at the particle-scale level (osmotic swelling and crystalline

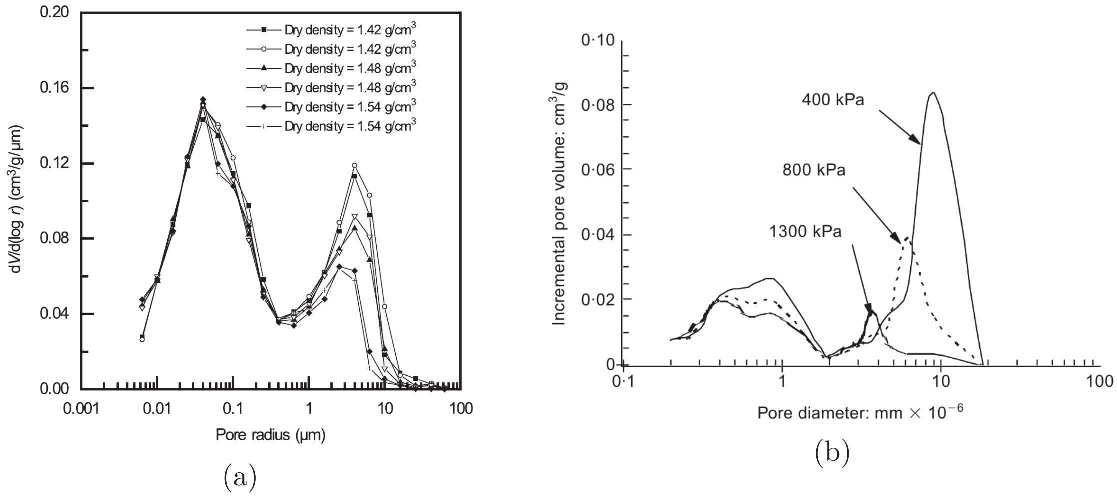

Figure 3: (a) Pore size density of compacted Guangxi expansive soil at various dry densities (Miao et al. 2007). (b) Microstructure of compacted kaolin after static compaction to different static pressures (Sivakumar et al., 2006).

swelling). This issue is discussed in more detail by (Mašín and Khalili 2012).

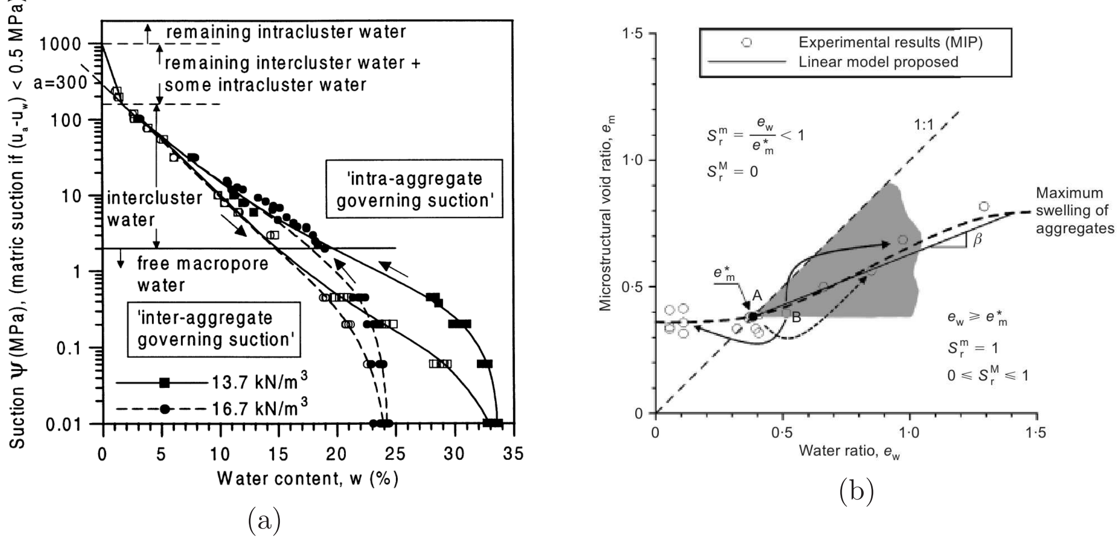

Figure 4: (a) Main wetting and drying water retention curves of Boom clay compacted to different densities (Romero et al. 1999). (b) Microstructural interpretation of the water retention behaviour of double structure soils by Romero et al. (2011).

Double structure of compacted soils is also evinced in their water retention behaviour, as put forward by Romero (1999) and Romero et al. (1999) and recently combined into a unified modelling framework by Romero et al. (2011). Fig. 4a shows water retention curves of a Boom clay compacted to two different initial densities. Clearly, water retention curves are independent of density in the high suction range. In this case, the water is retained inside the clay aggregates (macroporosity is dry). The results are thus consistent with the MIP results presented above (recall that the size of micropores was found to be independent of the compaction load). In the lower suction range, micropores are (thanks to smaller pore size and thus higher air entry value of suction) saturated, and the water retention behaviour is governed by the partially saturated macrostructure. As the water retention behaviour is, in general, dependent on porosity (Sun et al. 2008, Sun et al. 2007, Gallipoli et al. 2003, Nuth and Laloui 2008, Mašín 2010), so are the lower suction portions of water retention curves of double structure soils. Similar experimental results were obtained by Airò Farulla et al. (2011), who tested compacted scaly clay from Sicily. Conceptual interpretation of this behavior by Romero et al. (2011) is in Fig. 4b in terms of microstructural void ratio e^m (micropores volume over solid volume) vs. water ratio e_w (volume of water over solid volume). For e_w higher than a threshold value e^*_m (at the suction s^*_m) representing fully saturated micropores and dry macropores, the e^m changes with e_w along a line with slope β. $\beta = 0$ implies no aggregate swelling, whereas $\beta = 1$ implies maximum swelling in which aggregates fully occlude the macroporosity. β is for the given pore-fluid composition in the model considered as a soil-specific parameter.

3 Formalism for double structure coupling

3.1 Coupling of micro and macrostructural strain measures

In the case of no occlusion of macropores by the swelling aggregates, the following additive equation for the total strain rate $\dot{\boldsymbol{\epsilon}}$ holds true:

$$\dot{\boldsymbol{\epsilon}} = \dot{\boldsymbol{\epsilon}}^M + \dot{\boldsymbol{\epsilon}}^m \tag{1}$$

Here $\dot{\boldsymbol{\epsilon}}^m$ describes the deformation of the aggregates and $\dot{\boldsymbol{\epsilon}}^M$ measures the deformation of the macroskeleton. The three strain rates are coupled with rates of corresponding porosity measures, namely with the rates of total void ratio ($\dot{e}$), microvoid ratio ($\dot{e}^m$) and macrovoid ratio ($\dot{e}^M$) through

$$\frac{\dot{e}}{1+e} = \operatorname{tr}\dot{\boldsymbol{\epsilon}} \quad \text{(a)} \qquad \frac{\dot{e}^M}{1+e^M} = \operatorname{tr}\dot{\boldsymbol{\epsilon}}^M \quad \text{(b)} \qquad \frac{\dot{e}^m}{1+e^m} = \operatorname{tr}\dot{\boldsymbol{\epsilon}}^m \quad \text{(c)} \tag{2}$$

Khalili et al. (2010) demonstrated that the volume change of individual grains in soil skeleton imply no change of the skeletal void ratio (pore volume over solid volume), provided the skeleton configuration remains unchanged. It follows that, due to the grain swelling, the pore volume increases in the same fraction as solid volume to keep the void ratio constant. To be consistent with this observation, microvoid ratio e^m is defined as the ratio of micropore volume (V_p^m) over total solid volume (V_s), macrovoid ratio e^M is defined as the ratio of macropore volume (V_p^M) over the total volume of aggregates (V_A) and the total void ratio is $e = (V_p^m + V_p^M)/V_s$, as normal. Note that the usually adopted definition of $e^M = V_p^M/V_s$ (Gens et al. 2011, Sánchez et al. 2005), implying $e = e^M + e^m$, is not consistent with the above comment, as it leads to a nil change of V_p^M with the change of V_p^m. The definition of the porosity measures adopted in this work imply

$$e = e^M + e^m + e^M e^m \tag{3}$$

Water volume fractions of the two pore systems will be, consistently with the definition of void ratios, described by the total degree of saturation S_r (water volume V_w over V_p), microscopic degree of saturation S_r^m (water volume in micropores V_w^m over V_p^m) and macroscopic degree of saturation S_r^M (water volume in macropores V_w^M over V_p^M). The following relation then holds true

$$S_r = S_r^M + \frac{e^m}{e}(S_r^m - S_r^M) \tag{4}$$

Note that the adopted definition of S_r^M is equal to the "effective degree of saturation" S_r^e by Alonso et al. (2010).

So far, the deformation of macroskeleton and the deformation of aggregates were both fully contributing to the overall deformation. To include the possibility for the aggregates to occlude into the macropores, Eq. (1) is modified to

$$\dot{\boldsymbol{\epsilon}} = \dot{\boldsymbol{\epsilon}}^M + f_m \dot{\boldsymbol{\epsilon}}^m \tag{5}$$

where the factor $0 \leq f_m \leq 1$ quantifies the level of occlusion of macroporosity by aggregates. When $f_m = 1$, pure swelling or shrinking of aggregates implies the same global swelling or shrinking of the soil sample ($\dot{\boldsymbol{\epsilon}} = \dot{\boldsymbol{\epsilon}}^m$), with no change of macrovoid ratio and no skeletal rearrangement ($\dot{\boldsymbol{\epsilon}}^M = \mathbf{0}$). Contrary, $f_m = 0$ means that the aggregates freely penetrate or recede from the macropores while implying no global sample deformation ($\dot{\boldsymbol{\epsilon}} = \dot{\boldsymbol{\epsilon}}^M$ independently of $\dot{\boldsymbol{\epsilon}}^m$). With Eq. (5), Eqs. (2a) and (2c) are still valid, but not the Eq. (2b). Microstructure (aggregate) can penetrate macropores, and thus influence e^M. An updated form of Eq. (2b) reads

$$\frac{\dot{e}^M}{1 + e^M} = \mathrm{tr}\left[\dot{\boldsymbol{\epsilon}}^M + (f_m - 1)\dot{\boldsymbol{\epsilon}}^m\right] \tag{6}$$

It is the macroskeletal strain rate $\dot{\boldsymbol{\epsilon}}^M = \dot{\boldsymbol{\epsilon}} - f_m \dot{\boldsymbol{\epsilon}}^m$ which is to be controlled by the constitutive model for macrostructure, $\dot{\boldsymbol{\epsilon}}^m$ by the model for microstructure, and the factor f_m which quantifies the double-structural coupling.

3.2 Effective stress measures and constitutive relationships

As indicated in Sec. 1, the behaviour of the two structural levels will in this paper be considered separate (including the effective stress measures), and linked through relations from Sec. 3.1. The mechanical constitutive equations for the two structural levels then read, under full generality,

$$\dot{\boldsymbol{\sigma}}^M = \mathbf{G}^M(\boldsymbol{\sigma}^M, \boldsymbol{q}^M, \dot{\boldsymbol{\epsilon}}^M) \tag{7}$$

$$\dot{\boldsymbol{\sigma}}^m = \mathbf{G}^m(\boldsymbol{\sigma}^m, \boldsymbol{q}^m, \dot{\boldsymbol{\epsilon}}^m) \tag{8}$$

$\mathbf{G}^M$ stands for a constitutive model for macroskeleton, $\mathbf{G}^m$ for a constitutive model for microstructure and $\boldsymbol{\sigma}^M$ and $\boldsymbol{\sigma}^m$ are two corresponding effective stress measures. $\boldsymbol{q}^M$ and $\boldsymbol{q}^m$ are vectors of state variables, which typically include suction. The general expression for the effective stress for unsaturated *single porosity* media is due to Bishop (1959):

$$\boldsymbol{\sigma} = \boldsymbol{\sigma}^{net} - \mathbf{1}s\chi \tag{9}$$

with χ being the effective stress parameter. As the two structural levels are considered separately, each of them may be considered as ordinary unsaturated single porosity medium. For each of the structural levels we may thus write

$$\boldsymbol{\sigma}^M = \boldsymbol{\sigma}^{netM} - \mathbf{1}s^M\chi^M \tag{10}$$

$$\boldsymbol{\sigma}^m = \boldsymbol{\sigma}^{netm} - \mathbf{1}s^m\chi^m \tag{11}$$

A complete hydromechanical model for unsaturated soils requires also specification of a constitutive relationship for soil hydraulic behaviour (water retention model). In this case, the stress measure is represented by the value of suction. The corresponding strain-like quantities are the macrostructural and microstructural degrees of saturation respectively (S_r^M and S_r^m). The hydraulic constitutive relationships may be written as

$$\dot{S}_r^M = H^M(\dot{s}^M, s^M, \dot{\boldsymbol{\epsilon}}^M) \tag{12}$$

$$\dot{S}_r^m = H^m(\dot{s}^m, s^m, \dot{\boldsymbol{\epsilon}}^m) \tag{13}$$

with H^M and H^m being the water retention models for macrostructure and microstructure respectively. Note the coupling between the hydraulic and mechanical parts. The hydraulic models H^M and H^m depend on the mechanical strain measures $\dot{\boldsymbol{\epsilon}}^M$ and $\dot{\boldsymbol{\epsilon}}^m$. The mechanical models $\mathbf{G}^M$ and $\mathbf{G}^m$ may depend on the hydraulic strain measures S_r^M and S_r^m through the definition of the effective stress parameters χ^M and χ^m.

4 Model for expansive clays

Using formal model definition from Sec. 3, a complete hydromechanical model for double structure medium requires specification of the effective stress measures $\boldsymbol{\sigma}^M$ and $\boldsymbol{\sigma}^m$, constitutive relationships $\mathbf{G}^M$, $\mathbf{G}^m$, H^M and H^m, and the coupling function f_m. These will in this section be developed for the specific case of compacted expansive soils. The equations are limited to the ones needed for explanation of the proposed approach. A complete model formulation is described in Appendix.

4.1 Macrostructural effective stress $\boldsymbol{\sigma}^M$ and the water retention model for macrostructure H^M

The soils of the interest in this work, described in Sec. 2, have maximum aggregate sizes of the order of tens of micrometers (see Figs. 2 and 3). For such a material, it is reasonable to assume local hydraulic equilibrium between macro- and microstructure (Alonso et al. 1999), i.e. $s^m = s^M$. In addition, it is assumed that $\boldsymbol{\sigma}^{netM} = \boldsymbol{\sigma}^{netm}$. This equality is strictly valid only if the cross-sectional area of the aggregates is comparable to the cross-sectional area of the whole sample. Then,

$$\boldsymbol{\sigma}^M = \boldsymbol{\sigma}^{net} - \mathbf{1} s \chi^M \tag{14}$$

$$\boldsymbol{\sigma}^m = \boldsymbol{\sigma}^{net} - \mathbf{1} s \chi^m \tag{15}$$

It is recognised that this assumption is not valid for materials with bigger aggregate size, such as pellet material studied by Gens et al. (2011) and Alonso et al. (2011) or fissured material considered by Khalili et al. (2005).

For single porosity granular materials (sand, silt) and for aggregated materials with low to medium plasticity, the aggregates (respectively particles for single porosity media) are not substantially deformable when subject to stress and suction variation. The overall deformation of the soil skeleton is then governed by the deformation of macrostructure, i.e. $\dot{\boldsymbol{\epsilon}} = \dot{\boldsymbol{\epsilon}}^M$, $\dot{\boldsymbol{\sigma}} = \dot{\boldsymbol{\sigma}}^M$ and

$$\chi = \chi^M \tag{16}$$

Shear strength and compressibility of such soils has been studied by Khalili and Khabbaz (1998) and Khalili et al. (2004). They searched for such a formulation of χ which permitted to represent the rebound volumetric behaviour and shear strength in a unique effective stress space. They reached the following expression for the χ parameter:

$$\chi = \begin{cases} 1 & \text{for} \quad s < s_e \\ \left(\dfrac{s_e}{s}\right)^{\gamma} & \text{for} \quad s \geq s_e \end{cases} \tag{17}$$

in which s_e is a suction at air-entry or air-expulsion, depending whether drying or wetting process is considered respectively. γ is a soil parameter, which was found to be for a broad range of soils close to a unique value of $\gamma = 0.55$. In light of the above explanation, Eq. (17) may well be considered to represent the value of χ^M.

A similar approach as Khalili and Khabbaz (1998) and Khalili et al. (2004) has been adopted by Alonso et al. (2010). They suggested that the parameter χ is related only to the free water partially filling the macropores, and that immobile pore fluid within aggregates does not affect the macrostructural effective stress. Following thermodynamically consistent definition of the parameter $\chi = S_r$ derived using different approaches for single porosity medium (Coussy 2007, Houlsby 1997, Laloui et al. 2003, Lewis and Schrefler 1987, Hutter et al. 1999), Alonso et al. (2010) suggested equality[1]

$$\chi = S_r^M \tag{18}$$

They then demonstrated by studying critical shear strength and compressibility of different soils with aggregated structure that Eq. (18) successfully normalised the experimental data with respect to suction contribution.

[1] Note that the definition of S_r^M in this work equals to the "effective degree of saturation" S_r^e by Alonso et al. (2010)

Combination of Eqs. (16), (17) and (18) yields a Brooks and Corey (1964) type water retention model for macrostructure

$$S_r^M = \chi^M = \begin{cases} 1 & \text{for} \quad s < s_e \\ \left(\dfrac{s_e}{s}\right)^{\gamma} & \text{for} \quad s \geq s_e \end{cases} \tag{19}$$

In light of this interpretation, the Khalili and Khabbaz (1998) parameter γ represents a slope of the macrostructural water retention curve (WRC) in the $\ln S_r^M$ vs. $\ln s$ plane. In granular soils, WRC depends primarily on the soil grain size distribution (Fredlund et al. 2002). Then, somewhat peculiar uniqueness of the parameter γ may be implied by the fact that the shape of the aggregate-size-distribution of different compacted soils is actually similar. As a reference, see Figs. 2 and 3. They show pore-size distribution of double structure soil, which gives an indirect indication of the aggregate size distribution.

To account for the effects of hydraulic hysteresis, the macrostructural water retention model from Eq. (19) is enhanced as shown in Fig. 5. s_{en} is the air entry value during drying process and a_e is a model parameter representing ratio of the wetting branch air-expulsion value of suction s_{exp} and drying branch air-entry value of suction s_{en}. γ is the slope of WRC. It is here considered as a material-independent constant $\gamma = 0.55$ to simplify the model calibration procedure, but for the sake of generality it may be considered as a material parameter if needed. The slope of the macrostructure hydraulic scanning curve was deliberately selected as $\gamma/10$. Note that the interpretation of χ^M using Fig. 5 will be less accurate for hydraulic reversal paths, as evidenced experimentally by Khalili and Zargarbashi (2010).

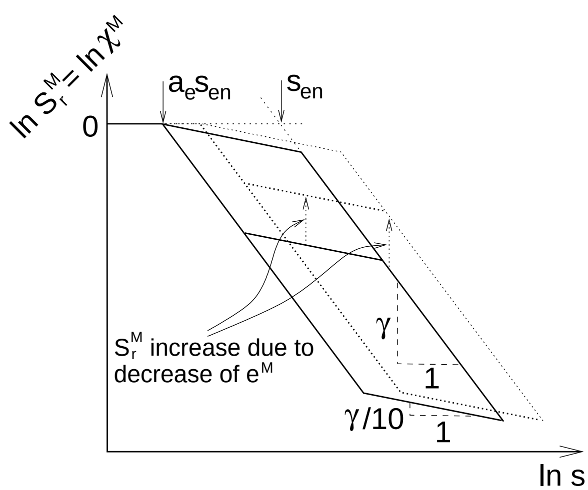

Figure 5: Water retention model for macrostructure.

Indeed, water retention curves are void ratio dependent (due to hydro-mechanical coupling), and this dependency must be considered in constitutive models to ensure accuracy of predictions (Sun et al. 2008, Sun et al. 2007, Gallipoli et al. 2003, Nuth and Laloui 2008, Mašín 2010, Wheeler et al. 2003). Mašín (2010) derived a water retention model, in which the void ratio dependency of WRC is implied by the adopted form of the effective stress tensor. The starting equation has originally been derived by Loret and Khalili (2000) from the assumption of existence of generalized elastic and plastic potentials. As detailed in Khalili et al. (2008), the existence of elastic potential $\mathbf{\Psi}(\boldsymbol{\sigma}, u_a, u_w)$, quadratic in $\boldsymbol{\sigma}$, but a priori not in suction, the elastic strain components are related to the stress components so that they enjoy the major symmetry. Considering also the irreversible components of pore water and pore air volume changes ($\dot{V}_w$ and $\dot{V}_a$), Khalili et al. (2008) finally derived

$$-\frac{\dot{V}_w}{V} = \psi\dot{\epsilon_v} - a_{11}\dot{u}_w - a_{12}\dot{u}_a \tag{20}$$

$$-\frac{\dot{V}_a}{V} = (1-\psi)\dot{\epsilon_v} - a_{21}\dot{u}_w - a_{22}\dot{u}_a \tag{21}$$

with constitutive constants a_{ij}. Rearrangement of the above equations, considering definitions of S_r and e, yields (Khalili et al. 2008)

$$\frac{\partial S_r}{\partial e} = \frac{\psi - S_r}{e} \tag{22}$$

where ψ is the effective stress rate parameter given by $\psi = \partial(\chi s)/\partial s$. Mašín (2010) adopted the χ expression from Eq. (17) in his developments, and the water retention curve was characterised by a slope λ_p in the $\ln S_r$ vs. $\ln s$ plane. The derivations yielded a relatively complex semi-analytical expression relating the air entry (expulsion) value of suction s_e and the WRC slope λ_p to void ratio. The only special case, in which the expression simplified, was when $\lambda_p = \gamma$. Then, the slope λ_p was independent of void ratio and the air entry value could be calculated explicitly as $s_e = s_{e0}e_0/e$, where s_{e0} represented the known value of the air entry suction at the reference void ratio e_0. Unfortunately, as λ_p was always found substantially lower than γ (which meant $\chi \neq S_r$), the special case could not be used to simplify the calculations. λ_p in the above represented the slope of the WRC expressed in global terms (total degree of saturation S_r).

In the present case, however, the above discussed assumption $\chi^M = S_r^M$ implies that the WRC slope λ^{pM} in *macro-structural terms* (S_r^M) coincides with γ. When the derivations by Mašín (2010) are repeated in terms of macrostructural quantities, the following expression for the air entry value of suction is obtained

$$s_{en} = s_{e0}\frac{e_0^M}{e^M} \tag{23}$$

with $\lambda^{pM} = \gamma$ independent of void ratio and of the applied suction. In Eq. (23) e_0^M is arbitrary reference macrovoid ratio and s_{e0} is the corresponding air-entry value of suction[2]. Apart from the parameter a_e (refer to Fig. 5), the adopted formulation for the macrostructure water retention curve does not require any other parameter. As sketched in Fig. 5, it is assumed (without direct exprimental evidence) that the change of e^M for states at the hydraulic scanning curve imposes the same change of S_r^M as if the state was on the main wetting or drying branch of WRC. In other words, "mechanical" wetting (or drying), in the sense defined by Tarantino (2009), does not change the relative position of a hydraulic state with respect to the main wetting and drying branches of WRCs.

[2]Note that in the present developments the microstructure has been considered as saturated, thus the superscript M has been omitted above s_{en} and s_{e0}

4.2 Macrostructural mechanical constitutive model $\mathbf{G}^M$

The mechanical behaviour of macroskeleton is described using a hypoplastic model for unsaturated soils by Mašín and Khalili (2008). The model has also been adopted as a reference model by Mašín and Khalili (2011), who enhanced it by the effects of temperature. In combination with the water retention model by Mašín (2010), the model was evaluated by D'Onza et al. (2011) in their benchmarking exercise on the performance of different hydromechanical models for unsaturated soils.

As other hypoplastic models, the model is based on a single incrementally non-linear (see Mašín et al. 2006) relationship relating the effective stress rate to rates of total strain rate and of suction. The model is based on the critical state soil mechanics (Gudehus and Mašín 2009), and implicitly predicts state boundary surface (Mašín and Herle 2005), similarly to other common elasto-plastic constitutive models based on the Cam-clay framework (Roscoe and Burland 1968). Unlike these models, however, the model predicts irreversible behaviour inside the state boundary surface, which gives it an important advantage in terms of its predictive capabilities (see D'Onza et al. 2011, Mašín 2012).

In terms of macrostructural quantities, the rate formulation of the model reads

$$\dot{\boldsymbol{\sigma}}^M = f_s \left(\boldsymbol{\mathcal{L}} : \dot{\boldsymbol{\epsilon}}^M + f_d \mathbf{N} \|\dot{\boldsymbol{\epsilon}}^M\| \right) + f_u \mathbf{H} \tag{24}$$

f_s, f_d and f_u are three scalar factors, $\boldsymbol{\mathcal{L}}$ is the fourth-order constitutive tensor and $\mathbf{N}$ and $\mathbf{H}$ are two second order constitutive tensors, all calculated in terms of $\boldsymbol{\sigma}^M$ in place of $\boldsymbol{\sigma}$ when compared to the original formulations. For their definition, see Appendix and the cited publications. The objective effective stress rate $\dot{\boldsymbol{\sigma}}^M$ is calculated from (14) as

$$\dot{\boldsymbol{\sigma}}^M = \dot{\boldsymbol{\sigma}}^{net} - \mathbf{1} \left[\frac{\partial(\chi^M s)}{\partial s} \dot{s} + \frac{\partial(\chi^M s)}{\partial e^M} \dot{e}^M \right] \tag{25}$$

which can be for the present case expressed as

$$\dot{\boldsymbol{\sigma}}^M = \dot{\boldsymbol{\sigma}}^{net} + \mathbf{1}\chi^M \left[(\gamma_a - 1)\dot{s} + \gamma s \frac{\dot{e}^M}{e^M} \right] \tag{26}$$

where $\gamma_a = \gamma$ for the states on the main drying and wetting branches of macrostructural WRC, $\gamma_a = \gamma/10$ for the states at the macrostructural hydraulic scanning curve and $\gamma_a = 0$ otherwise (for $s \leq s_{exp}$). $\dot{e}^M$ is calculated by Eq. (6).

Apart from the parameters of the macrostructural water retention curve (Sec. 4.1), the mechanical model requires altogether eight parameters. Five of them are parameters of the underlying model for saturated soils (Mašín 2005) (namely, N, λ^*, κ^*, φ_c and r), and they correspond to the parameters of the Modified Cam clay model. They are summarised in Sec. 4.6. Important parameters, which control the size of the state boundary surface, are N and λ^*. They represent position and slope of the isotropic normal compression line in the $\ln p^M$ vs. $\ln(1+e)$ plane, given by the expression due to Butterfield (1979). For a saturated soil,

$$\ln(1+e) = N - \lambda^* \ln(p^M/p_r) \tag{27}$$

with reference stress $p_r = 1$ kPa. In the model for unsaturated soils, $N(s)$ and $\lambda^*(s)$ depend on the current value of suction through the parameters n and l:

$$N(s) = N + n \ln\left(\frac{s}{s_e}\right) \qquad \lambda^*(s) = \lambda^* + l \ln\left(\frac{s}{s_e}\right) \tag{28}$$

where s_e is the value of the air entry/expulsion value of suction. This expression is adopted also in the proposed model. In order to keep consistency of the predictions with the hysteretic hydraulic model, however, the value of s_e is calculated from Eq. (19), leading to $s_e = s(S_r^M)^{(1/\gamma)}$. Note that the normal compression lines are still defined in terms of the global void ratio, as considering e^M in place of it would complicate the parameter calibration. For many soils, it is reasonable to assume, as a first approximation, the slopes of normal compression lines independent of suction, i.e. $l = 0$ (see Mašín and Khalili 2008 and Mašín and Khalili 2011).

The last parameter of the model m controls the influence of overconsolidation ratio (OCR) on magnitude of wetting-induced collapse. It is incorporated in the following way. In Eq. (24), the wetting-induced collapse is introduced by the tensor $\mathbf{H}$. It is multiplied by the factor f_u, which reads

$$f_u = \left(\frac{f_d}{f_d^{SBS}}\right)^{m/\alpha} \tag{29}$$

where α is a function of material parameters (see Appendix, Eq. (54)), f_d is the current value of the pyknotropy factor and f_d^{SBS} is its value at the state boundary surface. The factor f_d is in the model decreasing with increasing OCR, f_d^{SBS} thus represents maximum value of f_d for the current stress state. Eq. (29) therefore implies that f_u, and thus also the magnitude of wetting-induced collapse, decreases with increasing OCR. The rate of this decrease is controlled by m, in such a way that for $m = 0$ the collapse is always fully present independently of OCR, whereas for $m \rightarrow \infty$ the collapse occurs at the state boundary surface only.

4.3 Microstructural effective stress $\boldsymbol{\sigma}^m$, mechanical constitutive model $\mathbf{G}^m$ and water retention model H^m

To preserve certain simplicity of the model formulation, the microstructure is, thanks to its high air-entry value of suction, considered to be fully saturated. The microstructural water retention model thus reads simply

$$S_r^m = 1 \tag{30}$$

and the proposed model is considered not to be accurate for suctions higher then the microstructure air entry value of suction. The second assumption is that validity of the effective stress in the Terzaghi sense (see Sec. 2) is assumed. The microstructural effective stress is then governed through

$$\chi^m = S_r^m = 1 \tag{31}$$

this implies $\boldsymbol{\sigma}^m = \boldsymbol{\sigma}^{net} - \mathbf{1}s = \boldsymbol{\sigma}^{tot} + \mathbf{1}u_w$, i.e. the Terzaghi saturated effective stress. The above two assumptions have recently been supported by Mašín and Khalili (2012).

As demonstrated in Sec. 2, and as supported by Mašín and Khalili (2012), it is reasonable to assume the microstructure behaviour to be reversible. In this work, a simple volumetric model has been adopted:

$$\dot{\boldsymbol{\sigma}}^m = \mathbf{1}\frac{p^m}{\kappa_m}\operatorname{tr}\dot{\boldsymbol{\epsilon}}^m \tag{32}$$

This model yields linear response when represented in the $\ln p^m$ vs. $\ln(1+e^m)$ plane, i.e.

$$\ln(1+e^m) = C - \kappa_m \ln p^m \tag{33}$$

with a constant C. At the zero net mean stress, $p^m = s$ holds true. Reference microstructural void ratio e_r^m corresponding to an arbitrary reference value of suction s_r at zero net mean stress may be considered as material parameters, yielding explicit formulation for e^m:

$$e^m = \exp\left[\kappa_m \ln\frac{s_r}{p^m} + \ln(1+e_r^m)\right] - 1 \tag{34}$$

With an advantage, e^m and s_r may be considered equal to the microstructural void ratio (e_m^*) and suction (s_m^*) corresponding to the fully saturated micropores and dry macropores by Romero et al. (2011), but any other reference value of suction and corresponding e^m may be used.

4.4 Coupling function f_m

The last component in the proposed modelling framework is the coupling function f_m linking the responses of macrostructure and microstructure. Recall that this factor quantifies the level of occlusion of macroporosity by aggregates. When $f_m = 1$, pure swelling or shrinking of aggregates implies the same global swelling or shrinking of the soil. Contrary, $f_m = 0$ means that the aggregates freely penetrate or recede from the macropores while inducing no global sample deformation. As indicated in Sec. 2, the actual deformation mode depends on the level of compaction of macrostructure, which is measured by void ratio e. Minimum void ratio e_d corresponds to $e^M = 0$, i.e. $e_d = e^m$ (note that e^m varies with stress level, so also e_d is a variable). Maximum void ratio e_i corresponds to the state at the isotropic normal compression line. For the proposed model,

$$e_i = \exp\left[N(s) - \lambda^*(s)\ln p^M\right] - 1 \tag{35}$$

It is then convenient to define relative void ratio r_{em} as

$$r_{em} = \frac{e - e_d}{e_i - e_d} \tag{36}$$

For the densest possible state $r_{em} = 0$ and for the loosest possible state $r_{em} = 1$. Similar measure of the relative void ratio has been adopted by Gudehus (1996) and von Wolffersdorff (1996) in their hypoplastic models.

For aggregate swelling (wetting or unloading process) $f_m \to 1$ corresponds to a dense macrostructure (no macropore occlusion), whereas $f_m \to 0$ corresponds to a loose macrostructure (full occlusion of macropores by swelling aggregates). The following relationship satisfying these limiting properties has been adopted for $\dot{p}^m < 0$:

$$f_m = 1 - (r_{em})^{m_c} \tag{37}$$

where m_c is a model parameter controlling the influence of r_{em} on f_m for intermediate values of r_{em}. For particle shrinkage ($\dot{p}^m > 0$), $f_m = 0$ has always been assumed. In combination with the adopted macrostructural model (which predicts softer response in loading), higher values were found to lead to excessive global shrinkage.

The parameter m_c controls the influence of macrostructure compaction on the structural coupling. Similar influence, now on the structural collapse, has parameter m of the model for macrostructural behaviour. As the physical interpretation of the two parameters is similar, they are in the following assumed to take the same values ($m_c = m$). If needed, additional calibration freedom can be gained by their separate calibration.

4.5 Calculation of the model response in terms of global quantities $\dot{\boldsymbol{\epsilon}}$ and S_r

The constitutive models for the micro- and macrostructural levels enable to quantify the behaviour of each of the levels using properly selected existing constitutive models. However, the primary goal is to obtain the response in terms of global, directly measurable quantities. As for the mechanical models, the global strain rate is calculated from the macrostructural and microstructural strain rates using the set of equations (5), (7) and (8). To obtain the global water retention response, S_r is calculated from the known S_r^m and S_r^M and void ratios e^m and e using Eq. (4).

The solution of the system is for the proposed model straightforward for the known $\dot{\boldsymbol{\sigma}}^{net}$ and $\dot{s}$ (provided the solution is unique and exists). For the prescribed global strain rate $\dot{\boldsymbol{\epsilon}}$ and suction rate $\dot{s}$ the equations become implicit in $\dot{\boldsymbol{\sigma}}^{net}$, however. Eq. (24) can be with the aid of (1) written as

$$\dot{\boldsymbol{\sigma}}^M = f_s \left[\boldsymbol{\mathcal{L}} : (\dot{\boldsymbol{\epsilon}} - \dot{\boldsymbol{\epsilon}}^m) + f_d \mathbf{N} \|\dot{\boldsymbol{\epsilon}} - \dot{\boldsymbol{\epsilon}}^m\|\right] + f_u \mathbf{H} \tag{38}$$

where (from (32))

$$\dot{\boldsymbol{\epsilon}}^m = \mathbf{1} \kappa_m \frac{\dot{p}^m}{p^m} \tag{39}$$

and thus

$$\dot{\boldsymbol{\sigma}}^M = f_s \left[\boldsymbol{\mathcal{L}} : \left(\dot{\boldsymbol{\epsilon}} - \mathbf{1}\kappa_m \frac{\dot{p}^m}{p^m}\right) + f_d \mathbf{N} \left\|\dot{\boldsymbol{\epsilon}} - \mathbf{1}\kappa_m \frac{\dot{p}^m}{p^m}\right\|\right] + f_u \mathbf{H} \tag{40}$$

$\dot{\boldsymbol{\sigma}}^{net}$ appears in both the expressions for $\dot{\boldsymbol{\sigma}}^M$ and $\dot{p}^m$. Development of a robust and efficient numerical scheme to solve (40) is outside the scope of the present paper. For the sake of the present evaluation, the system was solved using a trial-and-error numerical procedure, in which the solution was approached by variation of the unknown $\dot{p}^m$. Such an approach is feasible as long as the microstructural behaviour is governed by a simple elastic volumetric model.

4.6 Summary of model parameters

In its simple form, the complete model for the expansive clays requires specification of 10 parameters:

- φ_c: Critical state friction angle.
- λ^*: Slope of normal compression lines (isotropic/oedometric/critical state line) of a saturated soil in the $\ln p^M/p_r$ vs $\ln(1+e)$ plane.
- N: Position of the isotropic normal compression line, i.e. the value of $\ln(1+e)$ for $p^M = p_r = 1$ kPa.
- κ^*: Slope of the *macrostructural* isotropic unloading line.
- r: Parameter controlling stiffness in shear.
- n: Parameter controlling the dependency of the position of the isotropic normal compression line on suction.
- m: Controls the dependency of wetting-induced collapse on the overconsolidation ratio and the macropore occlusion by microporosity on relative void ratio.
- κ_m: Specifies the dependency of microstructural swelling/shrinkage on the microstructural effective stress (i.e. saturated effective stress).
- s_{e0}: The air entry value of suction for the (arbitrary) reference macrostructural void ratio e_0^M.
- a_e: The ratio between the air expulsion and entry values of suction (controls the difference between the wetting and drying branches of water retention curves).

In addition, it is necessary to specify the initial values of the following state variables:

- e: global void ratio.
- e^m: microstructural void ratio. It may be advantageous to specify the initial value of e^m by means of Eq. (34), thus specify the value of e_r^m for the (arbitrary) reference value of suction s_r. A possible approach to initiation of e^m follows Romero et al. (2011). e_r^m is then equal to the water ratio e_w (and s_r is the corresponding suction) at which the macrostructure becomes dry in the drying test. At this value of suction, water retention curves for different global void ratios merge into a single curve (see Fig. 4 and the associated discussion). In the absence of relevant data, e^m should be calibrated using a trial-and-error procedure.
- S_r^M: The value of S_r^M is implied by the adopted water retention model for microstructure, but it is necessary to specify whether the current state belongs to the main drying branch of macrostructural WRC, main wetting branch or to the macrostructural scanning curve.

It is interesting to point out that, regardless the low number of material parameters, the model has advanced capabilities in predicting non-linear soil behaviour in compression and in shear, incorporates hysteretic water retention model coupled with the mechanical response, and predicts the inter-related behaviour of two structural levels. For comparison, the equivalent macrostructural model formed by a combination of the mechanical model by Mašín and Khalili (2008) and the water retention model by Mašín (2010) requires only one parameter less, but does not consider hysteretic water retention behaviour and double structure coupling. The pioneering and still popular model for expansive soils BExM by Alonso et al. (1999) requires 11 parameters and focuses on the mechanical response only.

5 Evaluation of the model

The model is evaluated using comprehensive experimental data set on unsaturated compacted Boom clay by Romero (1999), presented also in Romero et al. (1999) and Romero et al. (2011). The laboratory tests were performed on artificially prepared (dry side statically compacted) powder obtained from natural Boom clay. The soil is moderately swelling clay, containing 20-30% of kaolinite, 20-30% of illite and 10-20% of smectite. The liquid limit $w_L = 56\%$, plastic limit $w_P = 29\%$ and the amount of particles $< 2\mu$m is 50%. The testing program included two main soil packings of clay aggregates fabricated at a moulding water content of 15%: high porosity structure with collapsible tendency and low-porosity structure with swelling tendency (Romero et al. 1999).

To demonstrate the capabilities of the proposed approach, the predictions are compared with predictions by the existing (denoted as "original") model, which is formed by a combination of the mechanical model by Mašín and Khalili (2008) and the water retention model by Mašín (2010). Both the models were calibrated using the experimental data used also for the evaluation of the models, and all the predictions were obtained using a single parameter set with no further parameter manipulation. The data by Romero (1999) did not include the tests needed for calibration of parameters φ_c and r. They were calibrated using different data set on saturated Boom clay by Coop et al. (1995). The parameters are in Tabs. 1 and 2.

Table 1: *Parameters of the proposed hypoplastic model for expansive soils for Boom clay. Default values $\gamma = 0.55$ and $l = 0$ adopted. e_m initialised using $e_r^m = 0.38$ for $s_r = 2400$ kPa (from Romero et al. 2011).*

φ_c	λ^*	κ^*	N	r	n	m	κ_m	s_{e0} (e_0^M)	a_e
27°	0.08	0.008	1.05	0.4	0.025	2	0.04	200 kPa (0.18)	0.25

Table 2: *Parameters of the original hypoplastic model for Boom clay. Default values* $\gamma = 0.55$ *and* $l = 0$ *adopted.*

φ_c	λ^*	κ^*	N	r	n	m	λ_p	s_{e0} (e_0)
27°	0.08	0.008	1.05	0.4	0.025	2	0.17	70 kPa (0.75)

5.1 Unconfined wetting-drying tests

First, cyclic isotropic wetting-drying free swell test for three initial relative void ratios (loose, medium dense and dense soil) is simulated to demonstrate qualitative response of the model to cyclic loading. The model predictions for different values of the parameter m and constant value of $\kappa_m = 0.04$ are shown Fig. 6 in terms of the relative void ratio r_{em}. In all cases, the initially dense soil would accumulate swelling deformation during cyclic loading, and the initially loose soil would accumulate cyclic compaction. The model predicts the asymptotic cyclic state independent of further cycles. For given κ_m, the asymptotic state does not depend on the initial state, but on the value of the parameter m only.

The influence of the parameters m and κ_m on the asymptotic cyclic state is shown in Figs. 7a,b in terms of global void ratio. Although both the parameters influence the asymptotic state, the principle of their influence is fundamentally different – m controls wetting-induced collapsibility of macrostructure and macroporosity occlusion by aggregate swelling, whereas κ_m influence wetting-induced swelling of microstructure. This is clearly seen in Figs. 7c,d, where the results are plotted in terms of e^m and e^M.

It is interesting to point out that the asymptotic state in cyclic loading is predicted not only for suction cycles, but also for stress cycles in constant suction tests, even (but not only) in a saturated state. Fig. 8 shows the results of a saturated cyclic isotropic test on initially loose soil for two different values of the parameter m. The proposed model predicts asymptotic cyclic state, which depends on m. This strongly contrasts with predictions by the original model (in fact, for the saturated case the basic hypoplastic model for clays by Mašín 2005), which predicts continuous cyclic accumulation of compression. The proposed model thus does not suffer from volumetric rachetting, which is often regarded as one of the main drawbacks of hypoplasticity[3].

5.2 Constant volume wetting-drying tests

Fig. 9 demonstrates the difference between the water retention curves plotted in terms of global quantity S_r and macrostructural quantity S_r^M. The figure shows results of confined wetting-drying test with constant global void ratio e and variable net stress $\boldsymbol{\sigma}^{net}$ (for the evolution of $\boldsymbol{\sigma}^{net}$ in these tests, see Fig. 12 presented later). One test has been performed on a high porosity packing sample (denoted here as "loose sample" with $e = 0.932$), and

[3]Note that the model does not limit rachetting in shear, due to the purely volumetric model for microstructure.

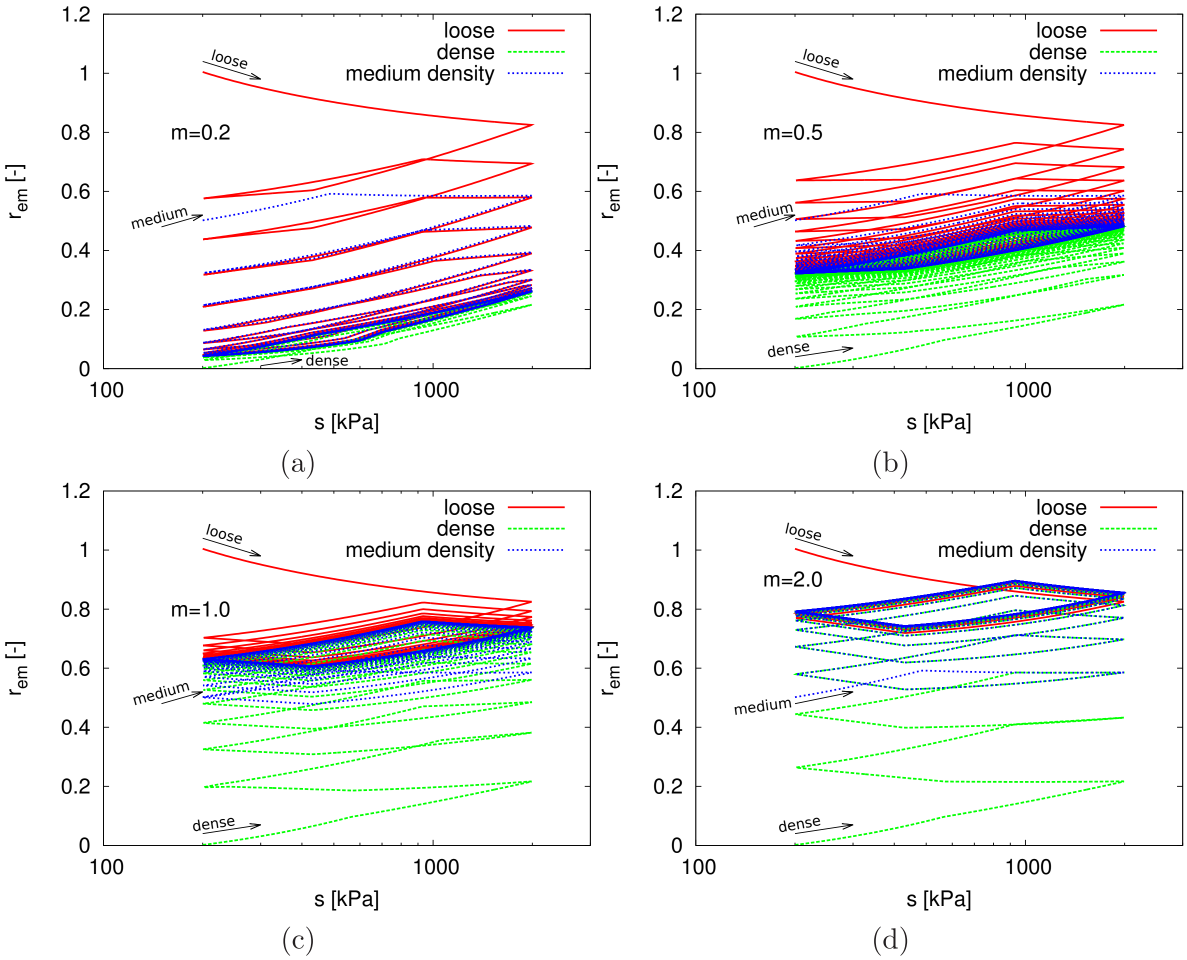

Figure 6: Response of the model to cyclic wetting-drying isotropic free swell test in terms of the relative void ratio r_{em} for different values of the parameter m.

one on a high density packing sample (denoted here as "dense sample" with $e = 0.65$). Both water retention curves have in terms of S_r^M similar slopes (controlled by $\gamma = 0.55$ and variation of e^M) and different air entry/expulsion values of suction (calculated by Eq. (23)). In terms of global quantity S_r, both water retention curves have different slopes, implied by the initial value of e_m and its variation with microstructural mean effective stress. The global water retention curves, which are controlled by the double structure coupling features of the model, agree well with the experimental data by Romero (1999), shown also in Fig. 9. Note that the modelled drying branches of WRCs in Fig. 9 represent results of a single constant volume wetting-drying experiments with the wetting branch terminated at s=450 kPa. This value of suction was sufficiently low to ensure compressive net stresses and constant volume conditions. The experimental data plotted in Fig. 9, on the other hand, are extrapolated from different test series for the given dry density, they could thus be plotted also in the higher suction range. For details of the extrapolation procedure, see Romero (1999).

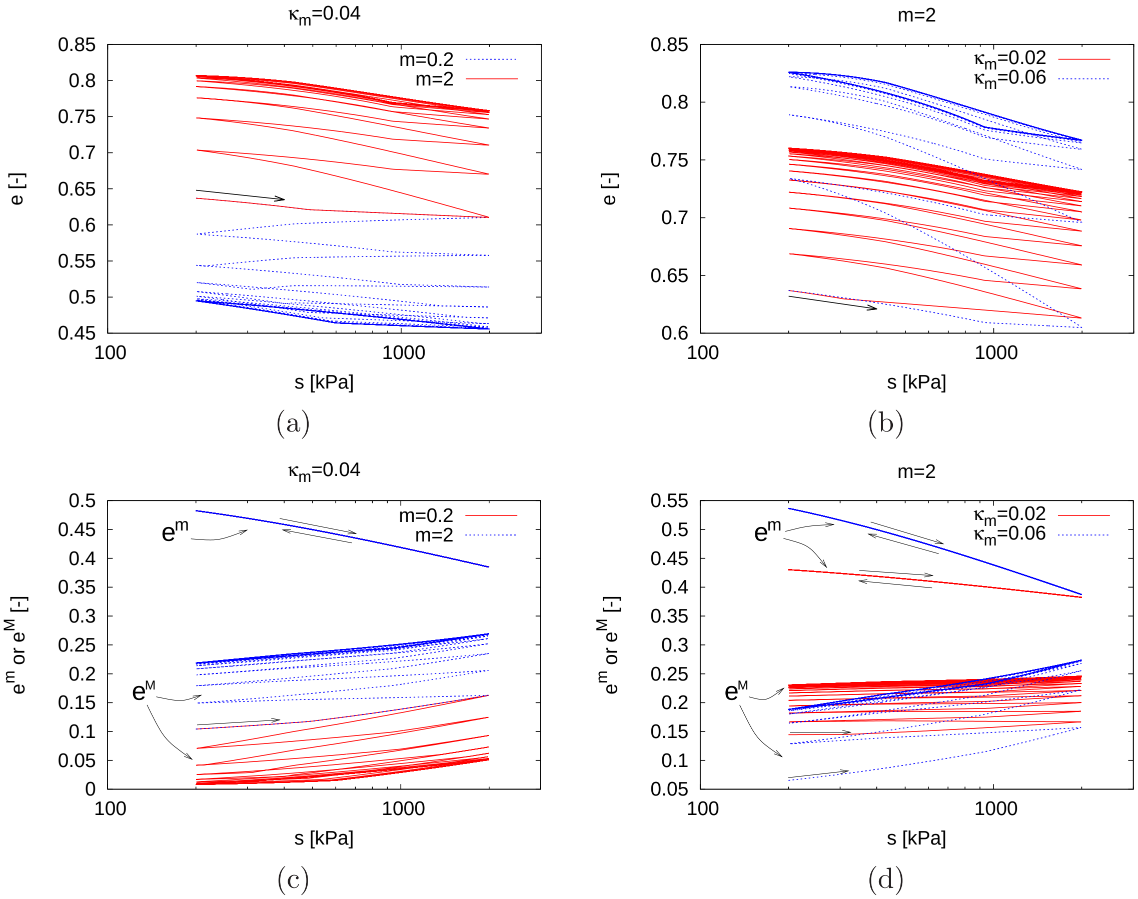

Figure 7: Response of the model to cyclic wetting-drying isotropic free swell test for medium dense soil and different values of parameter m (a,c) and κ_m (b,d). Results plotted in terms of global void ratio e (a,b) and e^m and e^M (c,d).

At this point, it is interesting to compare prediction of the proposed model with predictions by the original water retention model (Mašín 2010). In the original model, the slope of the global water retention curve is calibrated directly using parameter λ^p. The model then predicts the change of the slope of water retention curve and variability of the air expulsion value with void ratio using Eq. (22). Fig. 10 compares drying branches of water retention curves predicted by the original and proposed models for different global void ratios. Clearly, predictions by both models agree very closely. This once more supports the proposed coupling mechanisms.

It is also interesting to investigate the development of microstructural void ratio e^m during the tests. Fig. 11a shows that the model predicts reasonably correctly the water retention curves in terms of water ratio e_w (as in the case of Fig. 9, predictions of a single constant volume wetting-drying test are shown only). Fig. 11b shows development of e^m with e_w for different values of the parameter κ^m (loose sample). Experimental data by Romero et al. (2011) are

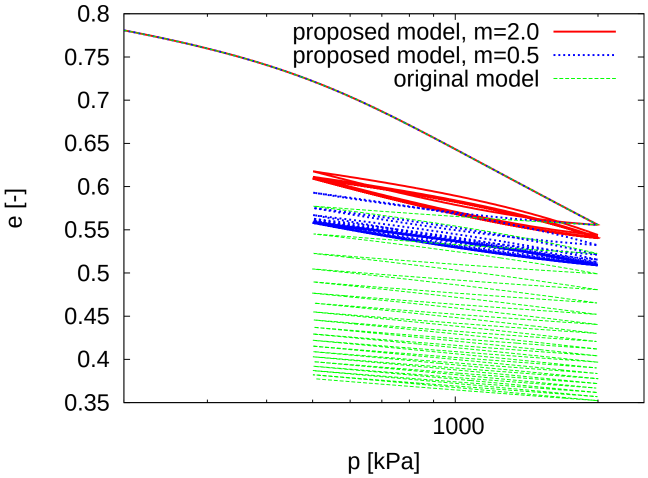

Figure 8: Response of the proposed and original models to cyclic isotropic test in a saturated state.

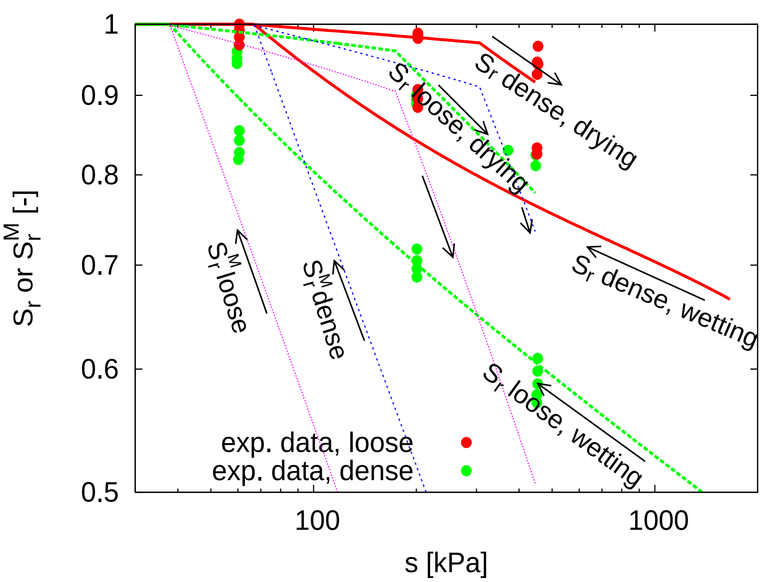

Figure 9: Constant global void ratio wetting-drying tests on Boom clay in terms of macrostructural degree of saturation S_r^M and a global quantity S_r. Experimental data by Romero (1999).

also included (taken from Fig. 4b). The parameter κ^m controls the development of e^m with e_w. It has thus the same effect as the parameter β of the model by Romero et al. (2011) (Fig. 4b). In the proposed model, this parameter has also a direct physical interpretation in terms of mechanical properties of microstructure. The parameter $\kappa^m = 0.04$, which was calibrated using results of oedometric swelling tests (Sec. 5.3), represents the data well,

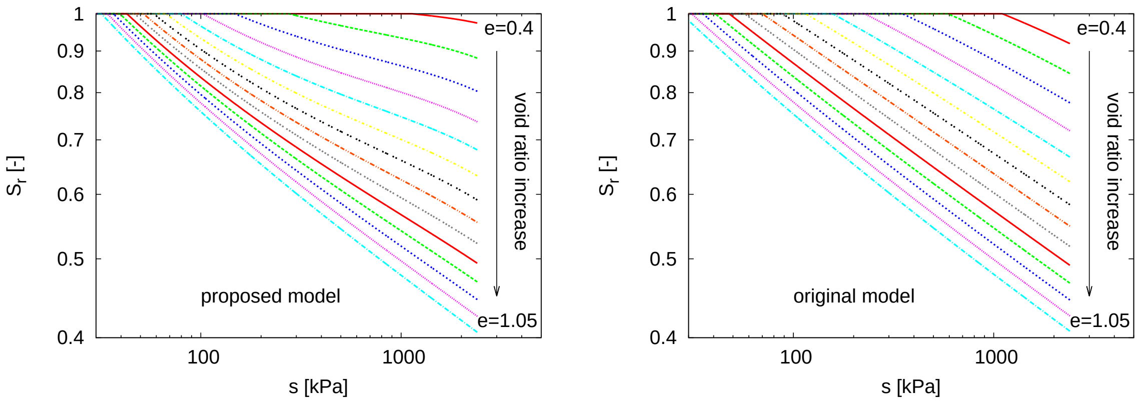

(a) (b)

Figure 10: The dependency of the drying branch of constant volume water retention curve on void ratio predicted by the proposed microstructural model (a) and original model (Mašín 2010) (b).

giving another argument towards validity of the proposed double structure hydromechanical coupling approach.

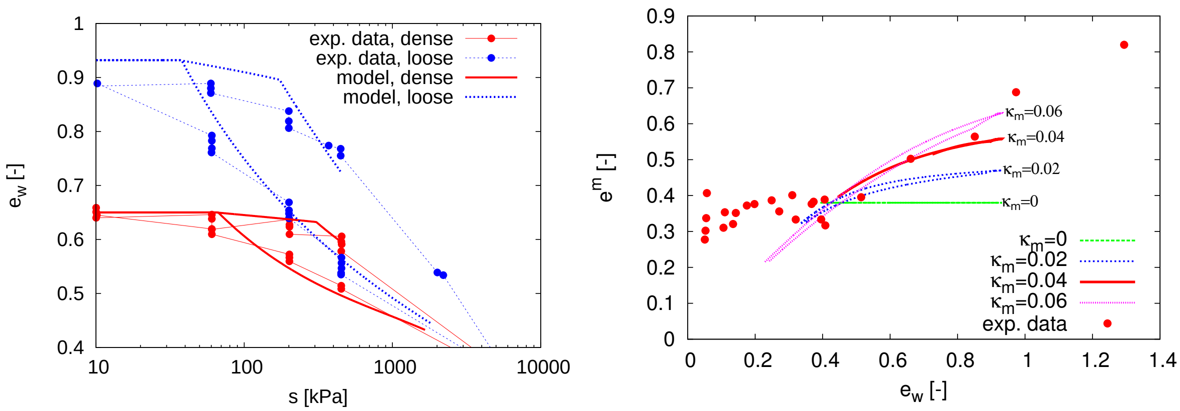

(a) (b)

Figure 11: Constant volume water retention curves (a) and demonstration of microstructural swelling in terms of e_w vs. e^m graph (b). Experimental data by Romero et al. (2011).

Confined swelling tests lead to a development of swelling pressures. The overall volumetric swelling is suppressed, and swelling of the aggregates occurs only to the extent allowed by the amount of occlusion of macropores. Fig. 12 shows development of horizontal and vertical net stresses with suction. Both the models predict correctly that higher swelling pressures reach the denser soil. However, the original model, which predicts swelling of macrostructure controlled by the macrostructural effective stress only, underpredicts the swelling pressure magnitude. The proposed model predicts the swelling pressures in a reasonable agreement with experiment, thanks to the additional contribution of the microstructural swelling.

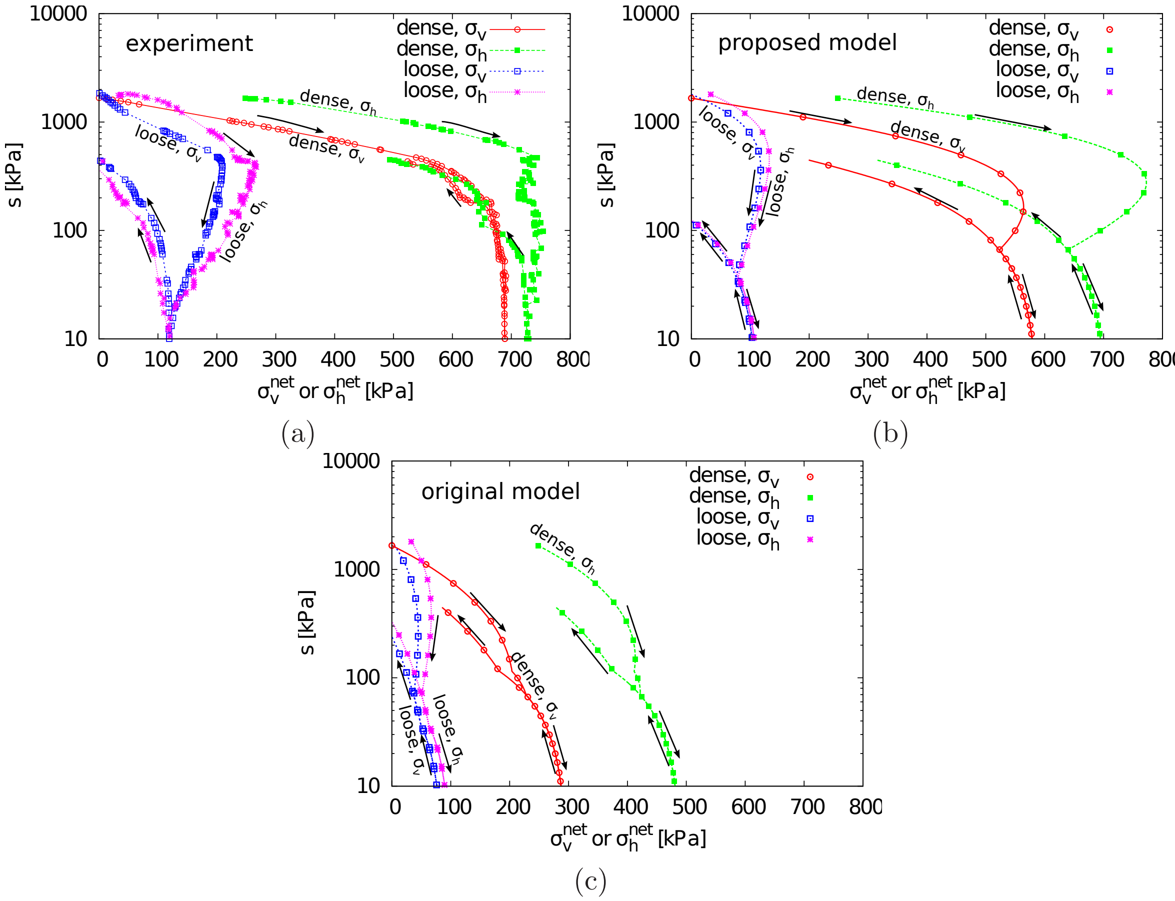

Figure 12: Development of swelling pressure with suction for denser and looser soil. Experimental data by Romero (1999) (a), compared with predictions by the proposed (b) and original (c) models.

5.3 Oedometric wetting-drying tests

Romero (1999) reported results of constant vertical net stress cyclic wetting-drying oedometric tests on samples with high porosity and high density fabric. The experimental results are in terms of suction vs. void ratio shown in Figs. 13a,c. As expected, and as described in Sec. 2, soil with the dense macrostructure is prone to accumulated swelling, whereas the soil with initially loose structure is prone to accumulated compaction. The amount of swelling/compaction also depends on the stress level. Predictions by the proposed model are shown in Figs. 13b,d. The model, in general, represents the experimental data very closely. The only more important qualitative discrepancy is that in the second wetting-drying cycles of the tests on dense soil at low vertical stresses (Figs. 13c,d), the model does not represent the hysteretic behaviour and thus slightly overpredicts the swelling strains. For comparison, Figs. 13e,f show predictions by the original model. Predictions of the tests on loose soil do not differ substantially from predictions by the proposed model. This is because the compaction behaviour (collapse of structure due to wetting) is primarily controlled by the stability of macrostructure, predicted the same by the original and proposed models. However, the results differ significantly in predictions of high density fabric tests. The original model predicts only minor swelling strains, implied by the adopted effective stress formulation. Contrary, the proposed model predicts the swelling behaviour relatively accurately, thanks to the predicted swelling of the aggregated microstructure. For completeness, Fig. 14 shows predictions of two tests in terms of degree of saturation. Clearly, also the hydraulic response is predicted reasonably well.

6 Summary and conclusions

A formalism for double structure hydromechanical coupling has been developed. An essential component of the model is independent modelling of the behaviour of microstructure and macrostructure (including separate effective stress measures), and considering hydromechanical coupling at both structural levels. Individual components of the general model have been selected to represent the behaviour of compacted expansive clays. Based on the recent findings by Alonso et al. (2010), a link between different effective stress measures from the literature has been suggested. Namely, the effective stress representation by Khalili and Khabbaz (1998) is considered to represent the macrostructural water retention model, following the approach by Alonso et al. (2010). It has been shown that using this assumption, formula from Mašín (2010) yields explicit and simple expression for the dependency of macrostructural water retention model on volumetric deformation of macroskeleton, simplifying substantially the model formulation.

Thanks to the insight into the physical phenomena controlling the global response of double structure soils, the proposed model has a small number of material parameters and state variables. Still the model has advanced capabilities in predicting the non-linear soil behaviour in compression and in shear, it incorporates hysteretic water retention model coupled with the mechanical response, and predicts the inter-related behaviour of two structural levels. Predictive capabilities of the model have been confirmed by simulation of comprehensive experimental data set on compacted Boom clay by Romero (1999) using a single set of material parameters.

An essential new component of the proposed model is representation of the microstructural mechanical behaviour controlled by the parameter κ_m. It has been shown that calibration of the parameter κ_m using volume change measured in swelling experiments leads to a correct global response in terms of degree of saturation, providing a support for the proposed coupling approach. Additional confidence is gained by equality of the predictions with the water retention model from Mašín (2010). Interestingly, the proposed approach have another substantial consequence on the global response of the model. It limits volumetric ratcheting, which is often regarded as one of the main drawbacks of hypoplasticity, the underlying mechanical model for macrostructure.

In summary, the proposed model is considered as an advance with respect to the existing hypoplastic model for unsaturated soils by Mašín and Khalili (2008) and Mašín (2010). Unlike the original model, the proposed model allows for predictions of soils with high plasticity. When the microstructural behaviour is switched-off (by considering zero microstructural volume change), the model reduces to the original model, while preserving its predictive capabilities and including hysteretic hydraulic response.

7 Acknowledgment

The author is delighted to have been invited by the organisation committee of the 2^{nd} European Conference on Unsaturated Soils to present this paper as a panel contribution. In addition, financial support by the research grants GACR P105/12/1705, TACR TA01031840 and MSM 0021620855 is greatly appreciated.

References

Airò Farulla, Battiato, A., C., and A. Ferrari (2011). The void ratio dependency of the retention behaviour for a compacted clay. In E. Alonso and A. Gens (Eds.), *Unsaturated Soils*, pp. 417–422. Taylor and Francis Group, London.

Airò Farulla, C., A. Ferrari, and E. Romero (2007). Mechanical behaviour of compacted scaly clay during cyclic controlled-suction testing. In T. Schanz (Ed.), *Springer Proceedings in Physics 112, Experimental Unsaturated Soil Mechanics*, pp. 345–354. Springer-Verlag Berlin.

Airò Farulla, C., A. Ferrari, and E. Romero (2010). Volume change behaviour of a compacted scaly clay during cyclic suction changes. *Canadian Geotechnical Journal 47*, 688–703.

Alonso, E. E., A. Loret, A. Gens, and D. Q. Yang (1995). Experimental behaviour of highly expansive double-structure clay. In 1^{st} *Int. Conference on Unsaturated Soils, Paris, France*, Volume 1, pp. 11–16. Balkema, Rotterdam.

Alonso, E. E., J.-M. Pereira, J. Vaunat, and S. Olivella (2010). A microstructurally based effective stress for unsaturated soils. *Géotechnique 60*(12), 913–925.

Alonso, E. E., E. Romero, and C. Hoffmann (2011). Hydromechanical behaviour of compacted granular expansive mixtures: experimental and constitutive study. *Géotechnique 61*(4), 329–344.

Alonso, E. E., J. Vaunat, and A. Gens (1999). Modelling the mechanical behaviour of expansive clays. *Engineering Geology 54*, 173–183.

Bagherieh, A. R., N. Khalili, G. Habibagahi, and A. Ghahramani (2009). Drying response and effective stress in a double porosity aggregated soil. *Engineering Geology 105*(1-2), 44–50.

Bishop, A. W. (1959). The principle of effective stress. *Teknisk Ukeblad 106*(39), 859–863.

Brooks, R. and A. Corey (1964). Hydraulic properties of porous media. *Hydrology paper No. 3, Colorado state University*.

Butterfield, R. (1979). A natural compression law for soils. *Géotechnique 29*(4), 469–480.

Coop, M. R., J. H. Atkinson, and R. N. Taylor (1995). Strength and stiffness of structured and unstructured soils. In *Proc.* 9^{th} *ECSMFE*, Volume 1, pp. 55–62.

Coussy, O. (2007). Revisiting the constitutive equations of unsaturated porous solids using a Lagrangian saturation concept. *International Journal for Numerical and Analytical Methods in Geomechanics 31*(15), 1675–1694.

Cui, Y. J., M. Yahia-Aissa, and P. Delage (2002). A model for the volume change behavior of heavily compacted swelling clays. *Engineering Geology 64*, 233–250.

Cuisinier, O. and L. Laloui (2004). Fabric evolution during hydromechanical loading of a compacted silt. *Canadian Geotechnical Journal 28*, 483–499.

Della Vecchia, G., C. Jommi, and E. Romero (2011). A fully coupled elastic-plastic hydromechanical model for compacted soils accounting for clay activity. *International Journal for Numerical and Analytical Methods in Geomechanics (in print) 61*.

D'Onza, F., D. Gallipoli, S. Wheeler, F. Casini, J. Vaunat, N. Khalili, L. Laloui, C. Mancuso, D. Mašín, M. Nuth, M. Pereira, and R. Vassallo (2011). Benchmark of constitutive models for unsaturated soils. *Géotechnique 61*(4), 283–302.

Fredlund, M. D., G. W. Wilson, and D. G. Fredlund (2002). Use of the grain-size distribution for estimation of the soil-water characteristic curve. *Canadian Geotechnical Journal 39*, 1103–1117.

Gallipoli, D., S. J. Wheeler, and M. Karstunen (2003). Modelling the variation of degree of saturation in a deformable unsaturated soil. *Géotechnique 53*(1), 105–112.

Gens, A. and E. Alonso (1992). A framework for the behaviour of unsaturated expansive clays. *Canadian Geotechnical Journal 29*, 1013–1032.

Gens, A., B. Vallején, M. Sánchez, C. Imbert, M. V. Villar, and M. van Geet (2011). Hydromechanical behaviour of a heterogeneous compacted soil: experimental observations and modelling. *Géotechnique 61*(5), 367–386.

Gudehus, G. (1996). A comprehensive constitutive equation for granular materials. *Soils and Foundations 36*(1), 1–12.

Gudehus, G. and D. Mašín (2009). Graphical representation of constitutive equations. *Géotechnique 52*(2), 147–151.

Houlsby, G. T. (1997). The work input to an unsaturated granular material. *Géotechnique 47*(1), 193–196.

Hutter, K., L. Laloui, and L. Vulliet (1999). Thermodynamically based mixture models for saturated and unsaturated soils. *Mechanics of Cohesive-Frictional Materials 4*, 295–338.

Khalili, N., F. Geiser, and G. E. Blight (2004). Effective stress in unsaturated soils: review with new evidence. *International Journal of Geomechanics 4*(2), 115–126.

Khalili, N., M. A. Habte, and S. Zargarbashi (2008). A fully coupled flow-deformation model for cyclic analysis of unsaturated soils including hydraulic and mechanical hystereses. *Computers and Geotechnics 35*(6), 872–889.

Khalili, N. and M. H. Khabbaz (1998). A unique relationship for χ for the determination of the shear strength of unsaturated soils. *Géotechnique 48*(2), 1–7.

Khalili, N., A. Uchaipichat, and A. A. Javadi (2010). Skeletal thermal expansion coefficient and thermo-hydro-mechanical constitutive relations for saturated porous media. *Mechanics of Materials 42*, 593–598.

Khalili, N., R. Witt, L. Laloui, L. Vulliet, and A. Koliji (2005). Effective stress in double porous media with two immiscible fluids. *Geophysical research letters 32*(15), Art. No. 15309.

Khalili, N. and S. Zargarbashi (2010). Influence of hydraulic hysteresis on effective stress in unsaturated soils. *Géotechnique 60*(9), 729–734.

Koliji, A., L. Vulliet, and L. Laloui (2008). New basis for the constitutive modelling of aggregated soils. *Acta Geotechnica 3*(1), 61–69.

Laloui, L., G. Klubertanz, and L. Vulliet (2003). Solid-liquid-air coupling in multiphase porous media. *International Journal for Numerical and Analytical Methods in Geomechanics 27*, 183–206.

Lewis, R. W. and B. A. Schrefler (1987). *The finite element method in the deformation and consolidation of porous media*. Wiley, Chichester.

Lloret, A. and M. V. Villar (2007). Advances on the knowledge of the thermo-hydro-mechanical behaviour of heavily compacted "FEBEX" bentonite. *Physics and Chemistry of the Earth 32*, 701–715.

Loret, B. and N. Khalili (2000). A three-phase model for unsaturated soils. *International Journal for Numerical and Analytical Methods in Geomechanics 24*, 893–927.

Mašín, D. (2005). A hypoplastic constitutive model for clays. *International Journal for Numerical and Analytical Methods in Geomechanics 29*(4), 311–336.

Mašín, D. (2010). Predicting the dependency of a degree of saturation on void ratio and suction using effective stress principle for unsaturated soils. *International Journal for Numerical and Analytical Methods in Geomechanics 34*, 73–90.

Mašín, D. (2012). Hypoplastic cam-clay model. *Géotechnique (in print)*.

Mašín, D. and I. Herle (2005). State boundary surface of a hypoplastic model for clays. *Computers and Geotechnics 32*(6), 400–410.

Mašín, D. and N. Khalili (2008). A hypoplastic model for mechanical response of unsaturated soils. *International Journal for Numerical and Analytical Methods in Geomechanics 32*(15), 1903–1926.

Mašín, D. and N. Khalili (2011). A thermo-mechanical model for variably saturated soils based on hypoplasticity. *International Journal for Numerical and Analytical Methods in Geomechanics (in print, DOI: 10.1002/nag.1058)*.

Mašín, D. and N. Khalili (2012). Swelling phenomena and effective stress in compacted expansive clays. *(submitted)*.

Mašín, D., C. Tamagnini, G. Viggiani, and D. Costanzo (2006). Directional response of a reconstituted fine grained soil. Part II: performance of different constitutive models. *International Journal for Numerical and Analytical Methods in Geomechanics 30*(13), 1303–1336.

Miao, L., S. L. Houston, Y. Cui, and J. Yuan (2007). Relationship between soil structure and mechanical behaviour for an expansive unsaturated clay. *Canadian Geotechnical Journal 44*, 126–137.

Monroy, R., L. Zdravkovic, and A. Ridley (2010). Evolution of microstructure in compacted London Clay during wetting and loading. *Géotechnique 60*(2), 105–119.

Najser, J., D. Mašín, and J. Boháč (2012). Numerical modelling of lumpy clay landfill. *International Journal for Numerical and Analytical Methods in Geomechanics 36*(1), 17–35.

Nuth, M. and L. Laloui (2008). Advances in modelling hysteretic water retention curve in deformable soils. *Computers and Geotechnics 35*(6), 835–844.

Romero, E. (1999). *Characterisation and thermo-hydro-mechanical behaviour of unsaturated Boom clay: an experimental study*. Ph. D. thesis, Universitat Polytécnica di Catalunya, Barcelona, Spain.

Romero, E., G. Della Vecchia, and C. Jommi (2011). An insight into the water retention properties of compacted clayey soils. *Géotechnique 61*(4), 313–328.

Romero, E., A. Gens, and A. Lloret (1999). Water permeability, water retention and microstructure of unsaturated compacted Boom clay. *Engineering Geology 54*, 117–127.

Romero, E. and P. H. Simms (2008). Microstructure investigation in unsaturated soils: A review with special attention to contribution of mercury intrusion porosimetry and enironmental scanning electron microscopy. *Geotechnical and Geological Engineering 26*, 705–727.

Roscoe, K. H. and J. B. Burland (1968). On the generalised stress-strain behaviour of wet clay. In J. Heyman and F. A. Leckie (Eds.), *Engineering Plasticity*, pp. 535–609. Cambridge: Cambridge University Press.

Sánchez, M., A. Gens, and L. Do Nascimento Guimarães (2005). A double structure generalised plasticity model for expansive materials. *International Journal for Numerical and Analytical Methods in Geomechanics 29*, 751–787.

Simms, P. H. and E. K. Yanful (2001). Measurement and estimation of pore shrinkage and pore distribution in a clayey till during soil-water-characteristic curve tests. *Canadian Geotechnical Journal 38*, 741–754.

Sivakumar, V., W. C. Tan, E. J. Murray, and J. D. McKinley (2006). Wetting, drying and compression characteristics of compacted clay. *Géotechnique 56*(1), 57–62.

Sun, D. A., D. Sheng, L. Xiang, and S. W. Sloan (2008). Elastoplastic prediction of hydro-mechanical behaviour of unsaturated soils under undrianed conditions. *Computers and Geotechnics 35*, 845–852.

Sun, D. A., D. Sheng, and Y. F. Xu (2007). Collapse behaviour of unsaturated compacted soil with different initial densities. *Canadian Geotechnical Journal 44*(6), 673–686.

Sun, W. and D. Sun (2011). Coupled modelling of hydro-mechanical behaviour of unsaturated compacted expansive soils. *International Journal for Numerical and Analytical Methods in Geomechanics (in print, DOI: 10.1002/nag.1036*.

Taibi, S., J. M. Fleureau, N. Bou-Bekr, M. I. Zerhouni, A. Benchouk, K. Lachgueur, and H. Souli (2011). Some aspects of the behaviour of compacted soils along wetting paths. *Géotechnique 61*(5), 431–437.

Tarantino, A. (2009). A water retention model for deformable soils. *Géotechnique 59*(9), 751–762.

Thom, R., R. Sivakumar, V. Sivakumar, E. J. Murray, and P. MacKinnon (2007). Pore size distribution of unsaturated compacted kaolin: the initial states and final states following saturation. *Géotechnique 57*(5), 469–474.

Thomas, H. R. and P. J. Cleall (1999). Inclusion of expansive clay behaviour in coupled thermo hydraulic mechanical models. *Engineering Geology 54*, 93–108.

Villar, M. V. (1999). Investigation of the behaviour of bentonite by means of suction-controlled oedometer tests. *Engineering Geology 54*, 67–73.

von Wolffersdorff, P. A. (1996). A hypoplastic relation for granular materials with a pre-defined limit state surface. *Mechanics of Cohesive-Frictional Materials 1*, 251–271.

Wheeler, S. J., R. S. Sharma, and M. S. R. Buisson (2003). Coupling of hydraulic hysteresis and stress-strain behaviour in unsaturated soils. *Géotechnique 53*, 41–54.

Yang, D. Q., E. E. Alonso, and H. Rahardjo (1998). Modelling the volumetric behaviour of an unsaturated expansive soil. In 2^{nd} *Int. Conference on Unsaturated Soils, Beijing, China*, Volume 2, pp. 249–254.

Appendix

The mathematical formulation of the proposed model for expansive soils is summarised in the following. The behaviour of two structural levels is linked through

$$\dot{\boldsymbol{\epsilon}} = \dot{\boldsymbol{\epsilon}}^M + f_m \dot{\boldsymbol{\epsilon}}^m \tag{41}$$

Different state variables are defined as $e = (V_p^m + V_p^M)/V_s$, $e^m = V_p^m/V_s$, $e^M = V_p^M/V_s$, $S_r = V_w/V_p$, $S_r^m = V_w^m/V_p^m$ and $S_r^M = V_w^M/V_p^M$. For definition of volume measures V_x^y see Sec. 3.1. The quantities are linked through

$$\frac{\dot{e}}{1+e} = \operatorname{tr}\dot{\boldsymbol{\epsilon}} \qquad \frac{\dot{e}^M}{1+e^M} = \operatorname{tr}\left[\dot{\boldsymbol{\epsilon}}^M + (f_m - 1)\dot{\boldsymbol{\epsilon}}^m\right] \qquad \frac{\dot{e}^m}{1+e^m} = \operatorname{tr}\dot{\boldsymbol{\epsilon}}^m \tag{42}$$

$$e = e^M + e^m + e^M e^m \tag{43}$$

$$S_r = S_r^M + \frac{e^m}{e}(S_r^m - S_r^M) \tag{44}$$

The behaviour of macrostructure is governed by

$$\dot{\boldsymbol{\sigma}}^M = f_s\left(\boldsymbol{\mathcal{L}} : \dot{\boldsymbol{\epsilon}}^M + f_d \mathbf{N}\|\dot{\boldsymbol{\epsilon}}^M\|\right) + f_u \mathbf{H} \tag{45}$$

$\boldsymbol{\sigma}^M$ is the macrostructural effective stress defined by

$$\boldsymbol{\sigma}^M = \boldsymbol{\sigma}^{net} - \chi^M s \mathbf{1} \tag{46}$$

The macrostructural effective stress parameter χ^M coincides with the macrostructural degree of saturation S_r^M, i.e.

$$S_r^M = \chi^M = \begin{cases} 1 & \text{for} \quad s < s_e \\ \left(\frac{s_e}{s}\right)^\gamma & \text{for} \quad s \geq s_e \end{cases} \tag{47}$$

where the drying branch of macrostructural WRC is described by $s_e = s_{en}$ and wetting branch by $s_e = s_{exp}$. These two quantities are linked by

$$s_{exp} = a_e s_{en} \tag{48}$$

where a_e is a model parameter and

$$s_{en} = s_{e0} \frac{e_0^M}{e^M} \tag{49}$$

with parameters s_{e0} and e_0^M and $\gamma = 0.55$. Within the hysteretic model, the rate of S_r^M is given by

$$\dot{S}_r^M = -\gamma_a \frac{S_r^M}{s}\dot{s} - \gamma \frac{S_r^M}{e^M}\dot{e}^M \tag{50}$$

where $\gamma_a = \gamma$ for the main wetting and drying branches of WRC, $\gamma_a = \gamma/10$ at the hydraulic scanning curve and $\gamma_a = 0$ for $s < s_{exp}$. Maximum value of S_r^M is limitted to 1. The macrostructural effective stress rate from Eq. (45) is given by

$$\dot{\boldsymbol{\sigma}}^M = \dot{\boldsymbol{\sigma}}^{net} + \mathbf{1}\chi^M \left[(\gamma_a - 1)\dot{s} + \gamma s \frac{\dot{e}^M}{e^M}\right] \tag{51}$$

with $\dot{e}^M$ calculated using Eq. (42)b. The fourth-order tensor $\boldsymbol{\mathcal{L}}$ is a hypoelastic tensor given by

$$\boldsymbol{\mathcal{L}} = 3\left(c_1 \boldsymbol{\mathcal{I}} + c_2 a^2 \hat{\boldsymbol{\sigma}}^M \otimes \hat{\boldsymbol{\sigma}}^M\right) \tag{52}$$

with $\hat{\boldsymbol{\sigma}}^M = \boldsymbol{\sigma}^M / \operatorname{tr} \boldsymbol{\sigma}^M$. The two scalar factors c_1 and c_2 are defined as:

$$c_1 = \frac{2\left(3 + a^2 - 2^\alpha a\sqrt{3}\right)}{9r} \qquad\qquad c_2 = 1 + (1 - c_1)\frac{3}{a^2} \tag{53}$$

where r is a model parameter and the scalars a and α are functions of the material parameters φ_c, λ^* and κ^*

$$a = \frac{\sqrt{3}\,(3 - \sin\varphi_c)}{2\sqrt{2}\sin\varphi_c} \qquad\qquad \alpha = \frac{1}{\ln 2}\,\ln\left[\frac{\lambda^* - \kappa^*}{\lambda^* + \kappa^*}\left(\frac{3 + a^2}{a\sqrt{3}}\right)\right] \tag{54}$$

The second-order tensor $\mathbf{N}$ is given by

$$\mathbf{N} = \boldsymbol{\mathcal{L}} : \left(Y \frac{\mathbf{m}}{\|\mathbf{m}\|}\right) \tag{55}$$

with the quantity Y

$$Y = \left(\frac{\sqrt{3}a}{3 + a^2} - 1\right)\frac{(I_1 I_2 + 9I_3)\left(1 - \sin^2\varphi_c\right)}{8 I_3 \sin^2\varphi_c} + \frac{\sqrt{3}a}{3 + a^2} \tag{56}$$

where the stress invariants are defined as

$$I_1 = \mathrm{tr}(\boldsymbol{\sigma}^M) \qquad I_2 = \frac{1}{2}\left[\boldsymbol{\sigma}^M : \boldsymbol{\sigma}^M - (I_1)^2\right] \qquad I_3 = \det(\boldsymbol{\sigma}^M)$$

$\det(\boldsymbol{\sigma}^M)$ is the determinant of $\boldsymbol{\sigma}^M$. The second-order tensor $\mathbf{m}$ is calculated by

$$\mathbf{m} = -\frac{a}{F}\left[\hat{\boldsymbol{\sigma}}^M + \mathrm{dev}\,\hat{\boldsymbol{\sigma}}^M - \frac{\hat{\boldsymbol{\sigma}}^M}{3}\left(\frac{6\hat{\boldsymbol{\sigma}}^M : \hat{\boldsymbol{\sigma}}^M - 1}{(F/a)^2 + \hat{\boldsymbol{\sigma}}^M : \hat{\boldsymbol{\sigma}}^M}\right)\right] \tag{57}$$

with the factor F

$$F = \sqrt{\frac{1}{8}\tan^2\psi_h + \frac{2-\tan^2\psi_h}{2+\sqrt{2}\tan\psi_h\cos 3\theta}} - \frac{1}{2\sqrt{2}}\tan\psi_h \tag{58}$$

where

$$\tan\psi_h = \sqrt{3}\left\|\mathrm{dev}\,\hat{\boldsymbol{\sigma}}^M\right\| \qquad \cos 3\theta = -\sqrt{6}\frac{\mathrm{tr}\left(\mathrm{dev}\,\hat{\boldsymbol{\sigma}}^M \cdot \mathrm{dev}\,\hat{\boldsymbol{\sigma}}^M \cdot \mathrm{dev}\,\hat{\boldsymbol{\sigma}}^M\right)}{\left[\mathrm{dev}\,\hat{\boldsymbol{\sigma}}^M : \mathrm{dev}\,\hat{\boldsymbol{\sigma}}^M\right]^{3/2}} \tag{59}$$

The *barotropy* factor f_s introduces the influence of the mean stress level

$$f_s = \frac{3p^M}{\lambda^*(s)}\left(3 + a^2 - 2^\alpha a\sqrt{3}\right)^{-1} \tag{60}$$

and the *pyknotropy* factor f_d incorporates the influence of the overconsolidation ratio.

$$f_d = \left(\frac{2p^M}{p_e}\right)^\alpha \qquad p_e = p_r \exp\left[\frac{N(s) - \ln(1+e)}{\lambda^*(s)}\right] \tag{61}$$

where $p_r = 1$ kPa is the reference stress. Values of $N(s)$ and $\lambda^*(s)$ are represented by

$$N(s) = N + n\left\langle \ln\frac{s}{s_e}\right\rangle \qquad \lambda^*(s) = \lambda^* + l\left\langle \ln\frac{s}{s_e}\right\rangle \tag{62}$$

N, λ^*, n and l are model parameters and

$$s_e = s(S_r^M)^{(1/\gamma)} \tag{63}$$

The tensorial term $\mathbf{H}$ from Eq. (45) reads

$$\mathbf{H} = -c_i\frac{\boldsymbol{\sigma}^M}{s\lambda^*(s)}\left[n - l\ln\frac{p_e}{p_r}\right]\langle -\dot{s}\rangle \tag{64}$$

for $s > s_{exp}$ and $S_r < 1$, and $\mathbf{H} = \mathbf{0}$ otherwise. The factor c_i reads

$$c_i = \frac{3 + a^2 - f_d a\sqrt{3}}{3 + a^2 - f_d^{SBS} a\sqrt{3}} \tag{65}$$

f_d^{SBS} is the value of the pyknotropy factor f_d for states at the SBS, defined as

$$f_d^{SBS} = \|f_s\boldsymbol{\mathcal{A}}^{-1} : \mathbf{N}\|^{-1} \tag{66}$$

where the fourth-order tensor $\boldsymbol{\mathcal{A}}$ is expressed by

$$\boldsymbol{\mathcal{A}} = f_s\boldsymbol{\mathcal{L}} + \frac{1}{\lambda^*(s)}\boldsymbol{\sigma}^M \otimes \mathbf{1} \tag{67}$$

The factor controlling the collapsible behaviour f_u reads

$$f_u = \left(\frac{f_d}{f_d^{SBS}}\right)^{m/\alpha} \tag{68}$$

with m being a model parameter.

The behaviour of microstructure is governed by

$$\dot{\boldsymbol{\sigma}}^m = \mathbf{1}\frac{p^m}{\kappa_m}\,\mathrm{tr}\,\dot{\boldsymbol{\epsilon}}^m \tag{69}$$

where κ_m is a model parameter and $\boldsymbol{\sigma}^m$ is the microstructural effective stress given by

$$\boldsymbol{\sigma}^m = \boldsymbol{\sigma}^{net} - s = \boldsymbol{\sigma}^{tot} + u_w \tag{70}$$

The value of e^m may be initialised through

$$e^m = \exp\left[\kappa_m \ln \frac{s_r}{p^m} + \ln(1 + e_r^m)\right] - 1 \tag{71}$$

with parameters e_r^m and s_r.

Finally, the coupling function f_m reads

$$f_m = 1 - (r_{em})^m \tag{72}$$

for $\dot{p}^m < 0$ and $f_m = 0$ otherwise. r_{em} is relative void ratio

$$r_{em} = \frac{e - e_d}{e_i - e_d} \tag{73}$$

with

$$e_i = \exp\left[N(s) - \lambda^*(s) \ln p^M\right] - 1 \tag{74}$$

and

$$e_d = e_m \tag{75}$$

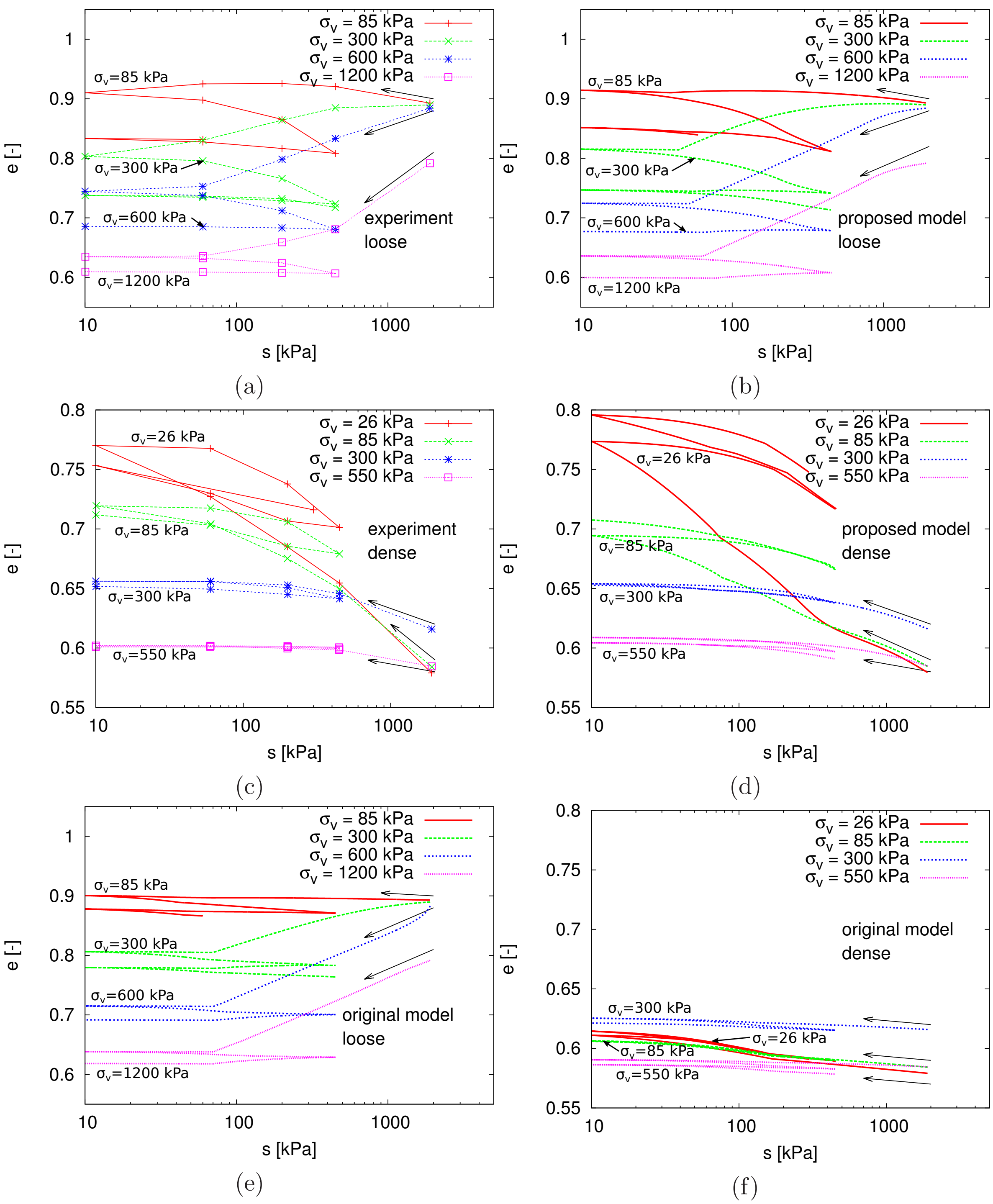

Figure 13: Constant σ_v^{net} wetting-drying oedometric experiments on Boom clay with loose and dense structures. Experimental data by Romero (1999) (a,c) compared with predictions by the proposed (b,d) and original (e,f) models.

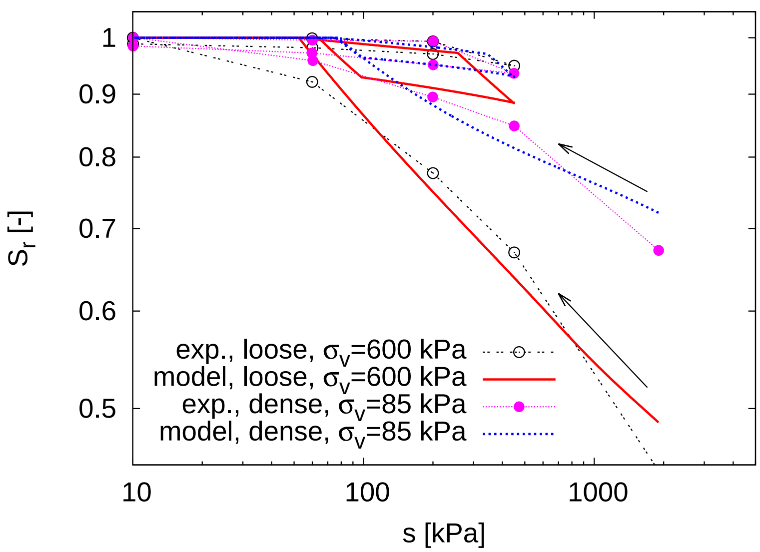

Figure 14: Constant σ_v^{net} wetting-drying oedometric experiments on Boom clay with loose and dense structures in terms of s vs. S_r. Experimental data by Romero (1999).